SUPPORTING INFORMATION

for

Perylene diimide–Cu^{2+} based fluorescent nanoparticles for detection of spermine in clinical, food samples: A step toward development of diagnostic kit as POCT tool for spermine

Kapil Kumar[a], Sandeep Kaur[b], Satwinderjit Kaur[b], Gaurav Bhargava[c], Subodh Kumar[a] Prabhpreet Singh[a*]

[a]Department of Chemistry, UGC Centre for Advanced Studies-II, Guru Nanak Dev University, Amritsar (Pb) 143 005, India. e-mail: prabhpreet.chem@gndu.ac.in; Tel: +91-84271-01534

[b]Department of Botanical and Environmental Sciences, Guru Nanak Dev University, Amritsar (Pb) 143 005, India

[c]Department of Chemical Sciences, IK Gujral Punjab Technical University, Kapurthala-144601, Punjab, India.

1. Spectroscopic analysis of EA-PDI and DGA-PDI

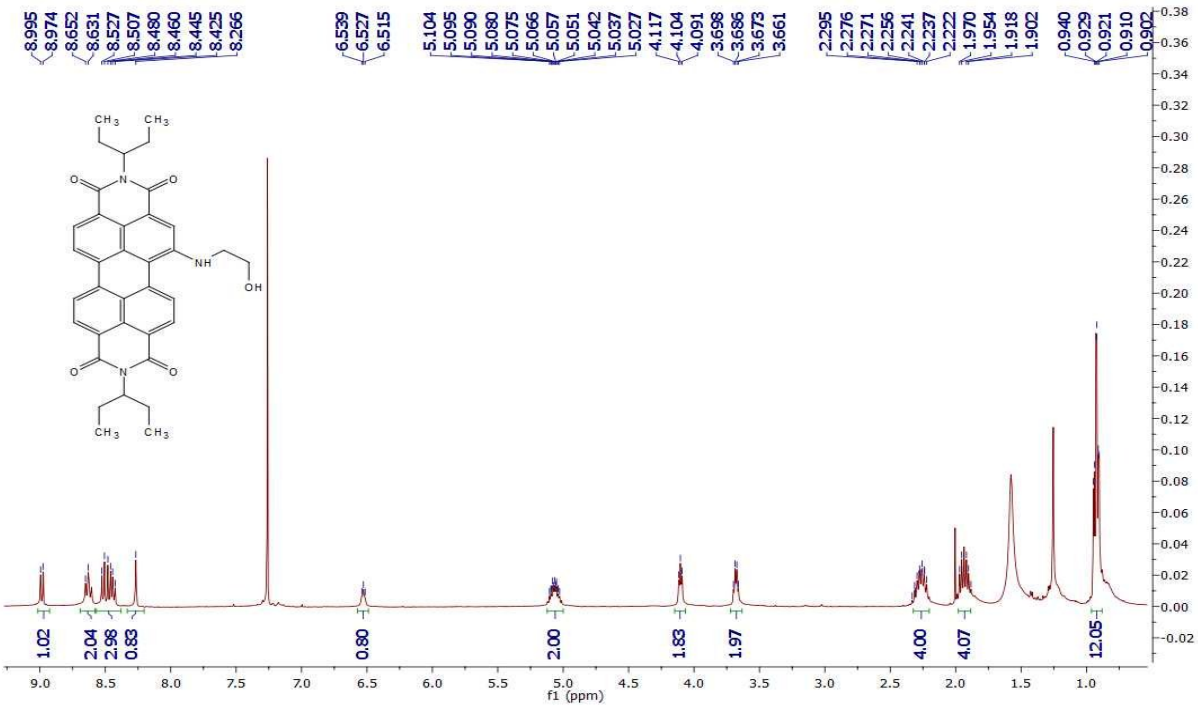

Figure S1a: ^{1}H NMR spectrum of **EA-PDI**.

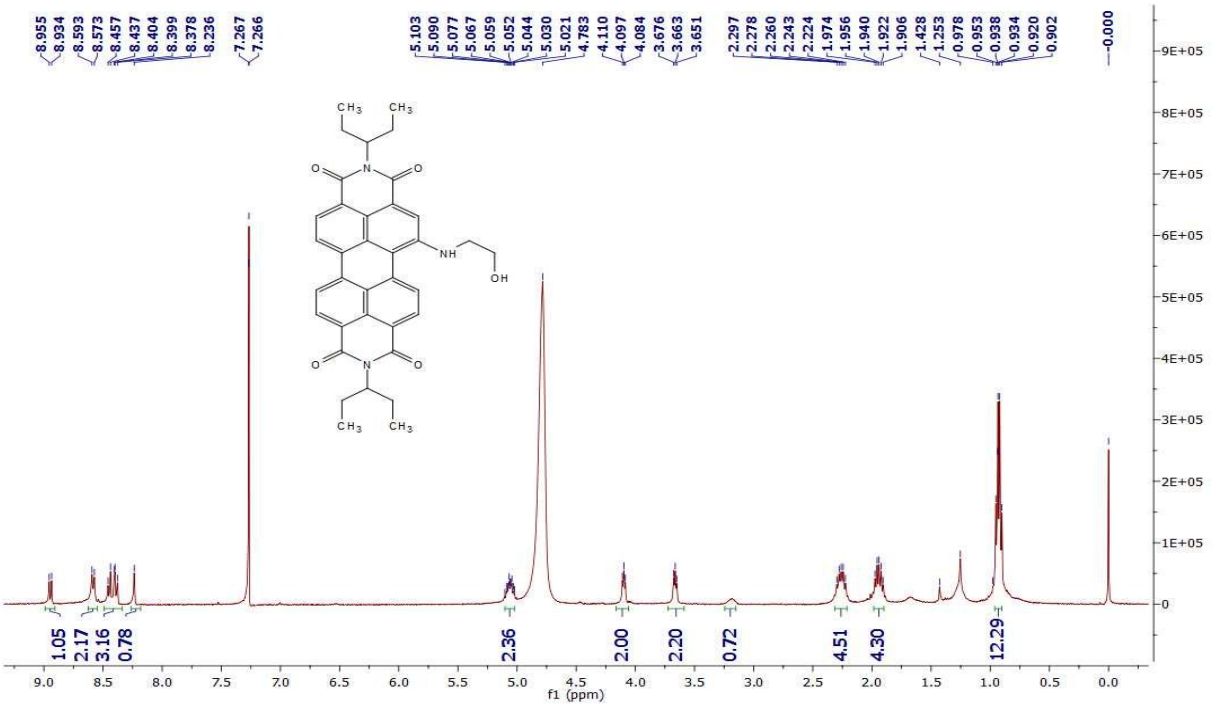

Figure S1b: ^{1}H NMR spectrum of **EA-PDI** after D_2O exchange.

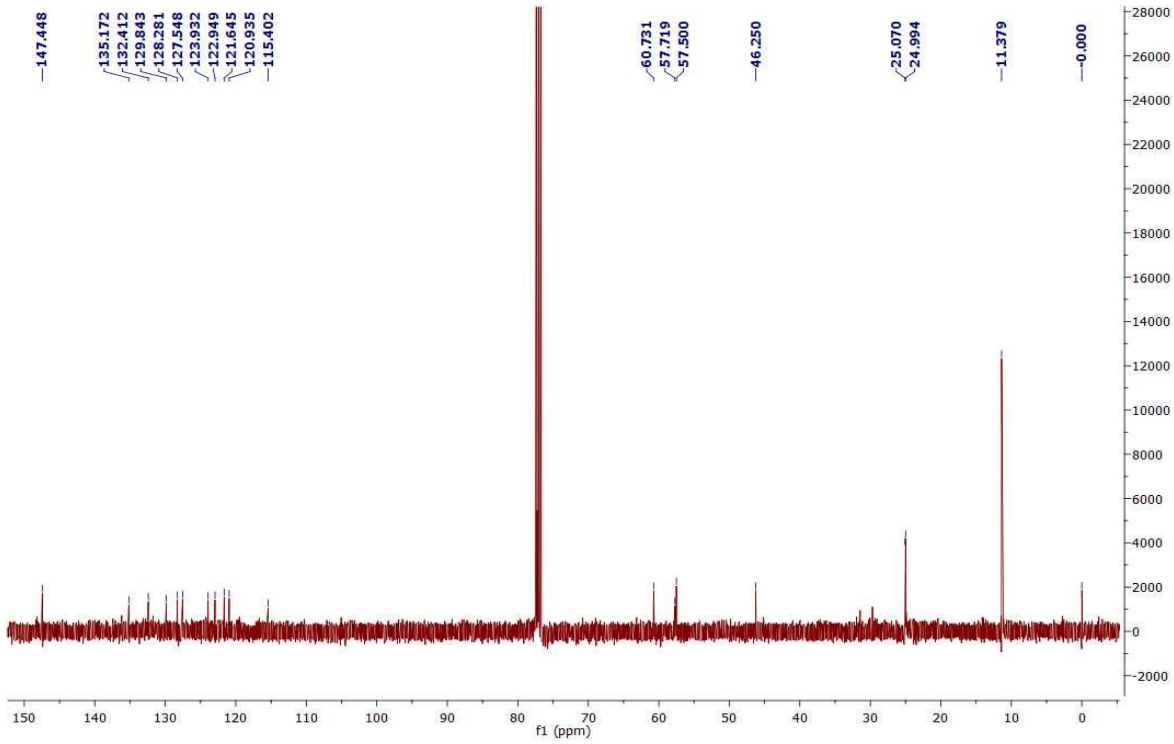

Figure S1c: ^{13}C NMR spectrum of **EA-PDI**.

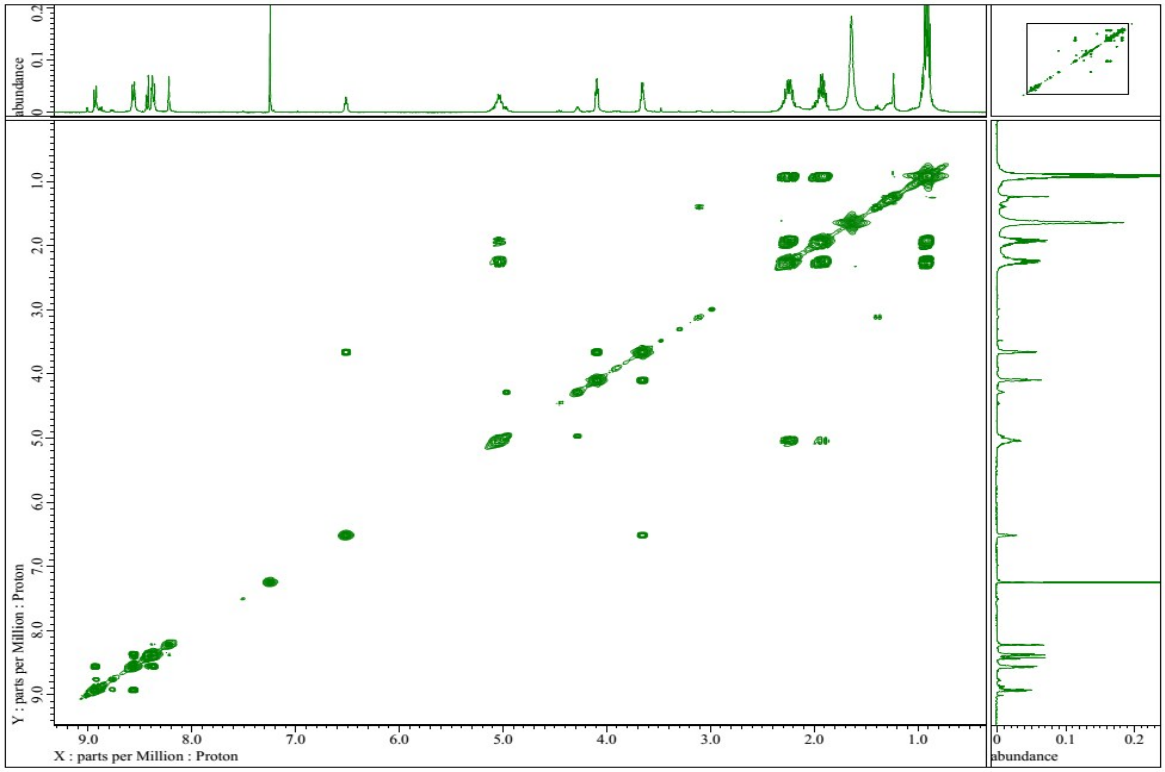

Figure S1d: ^{1}H-^{1}H COSY spectrum of **EA-PDI**.

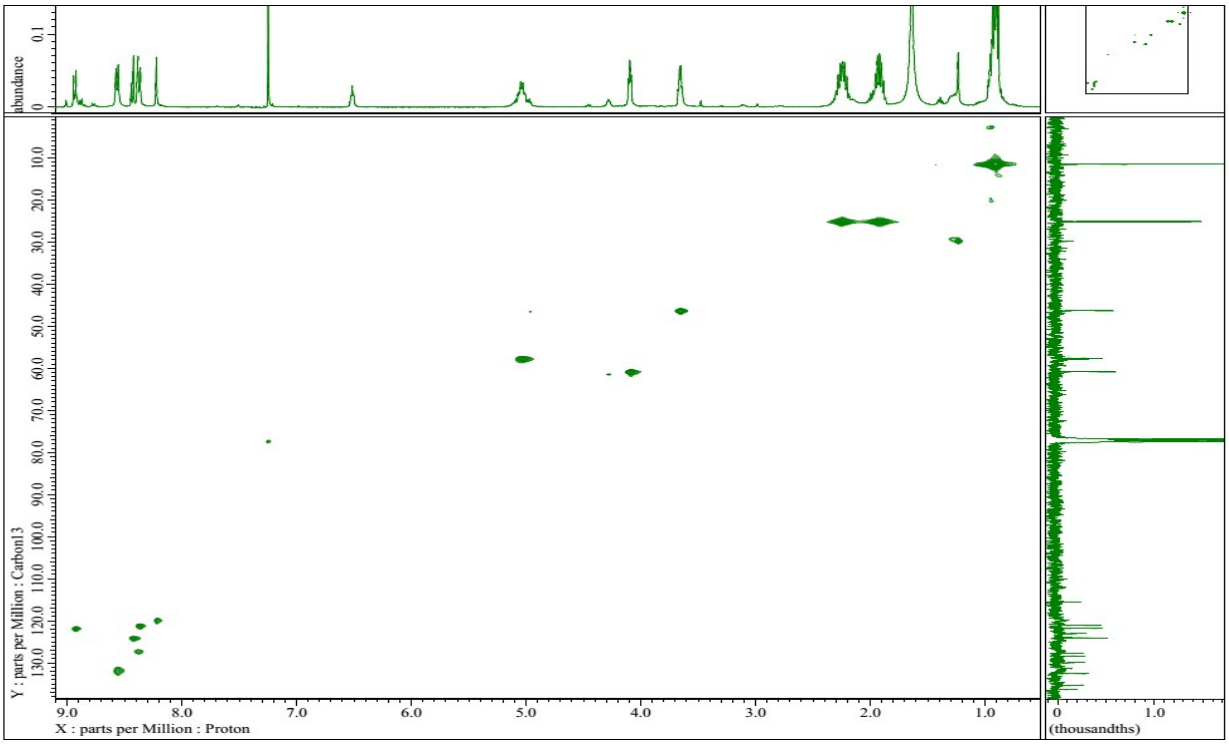

Figure S1e: HSQC spectrum of **EA-PDI**.

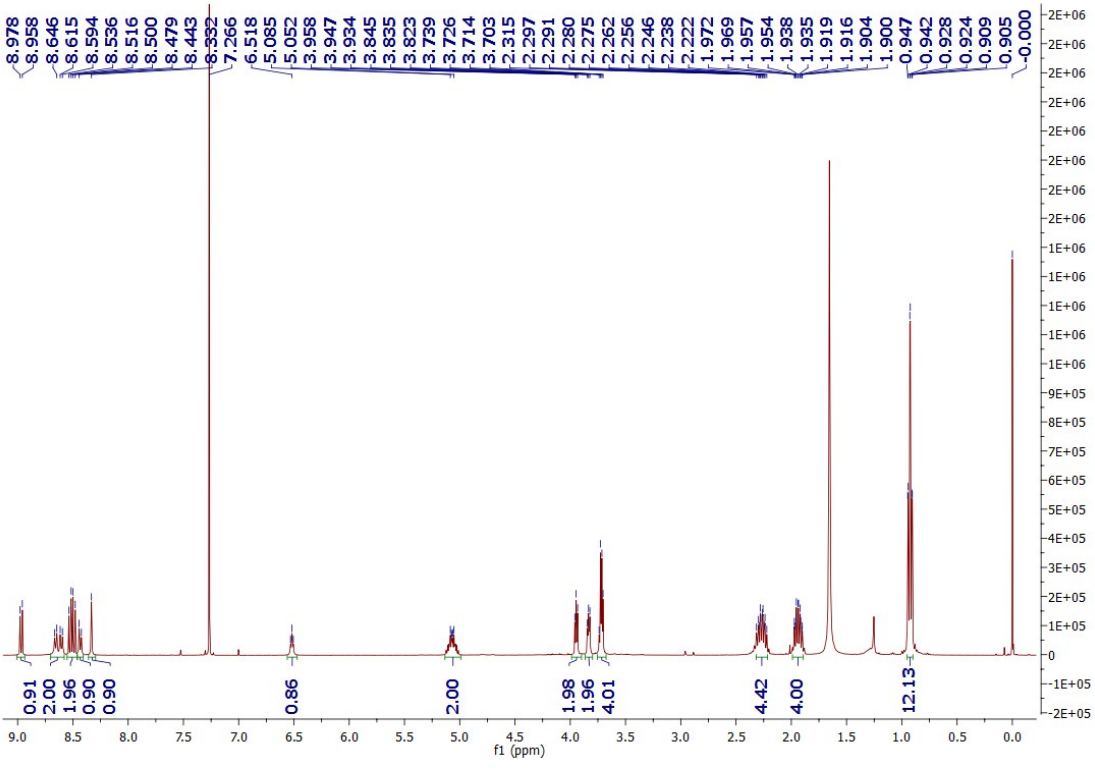

Figure S2a: ^{1}H NMR spectrum of **DGA-PDI**.

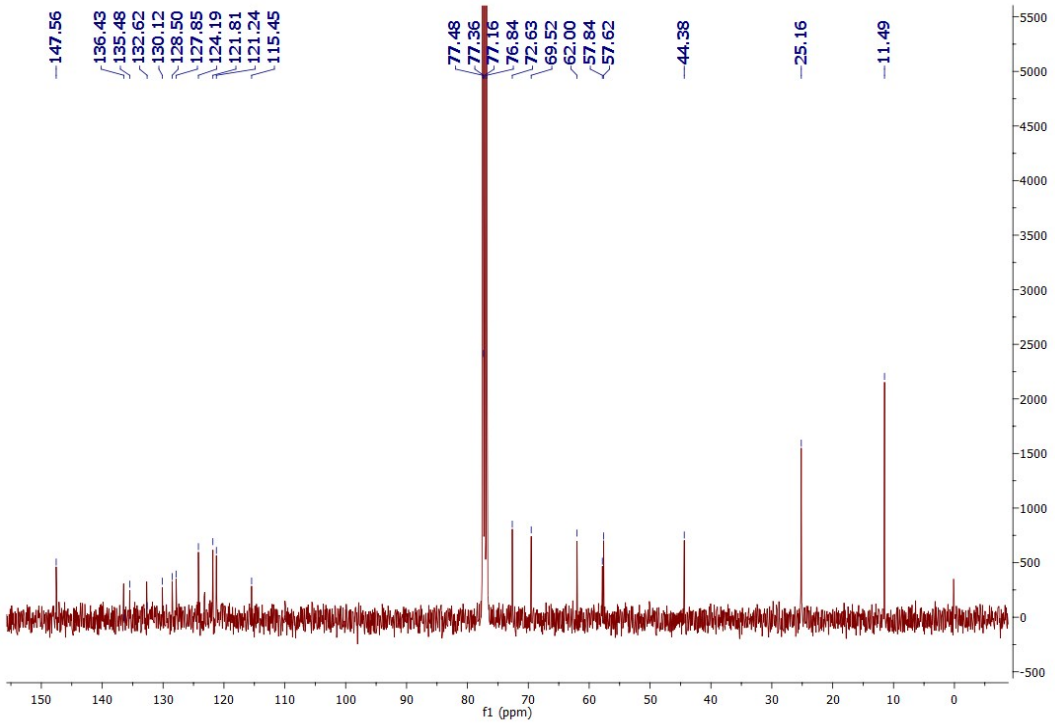

Figure S2b: ^{13}C NMR spectrum of **DGA-PDI**.

2. Cyclic Voltammetric studies of EA-PDI

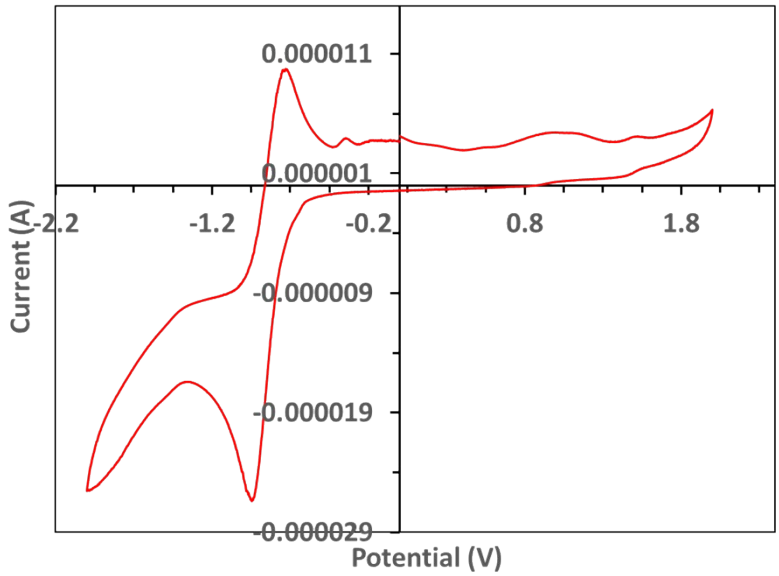

Figure S3: Cyclic voltammogram of **EA-PDI** recorded in dichloromethane (*vs.* Ag/AgCl).

3. Density Functional Theory (DFT) studies of EA-PDI

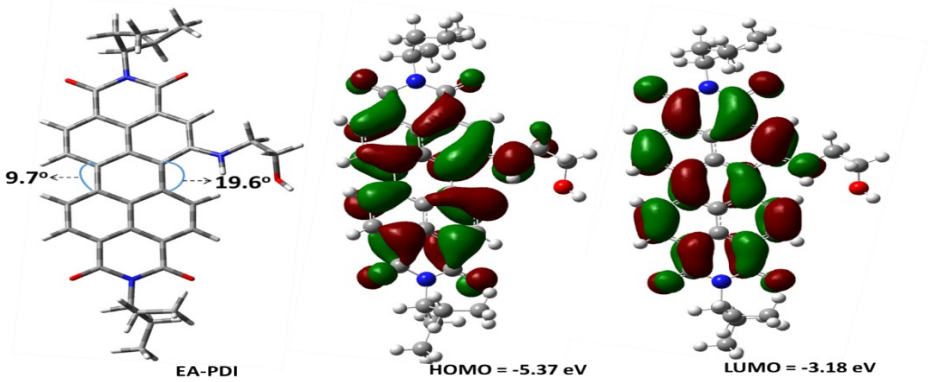

Figure S4: Molecular orbital analysis of **EA-PDI** with HOMO and LUMO presentation and energy optimized structure of **EA-PDI** showing twisting of naphthalene core.

4. Spectroscopic response of EA-PDI towards Cu^{2+} ions

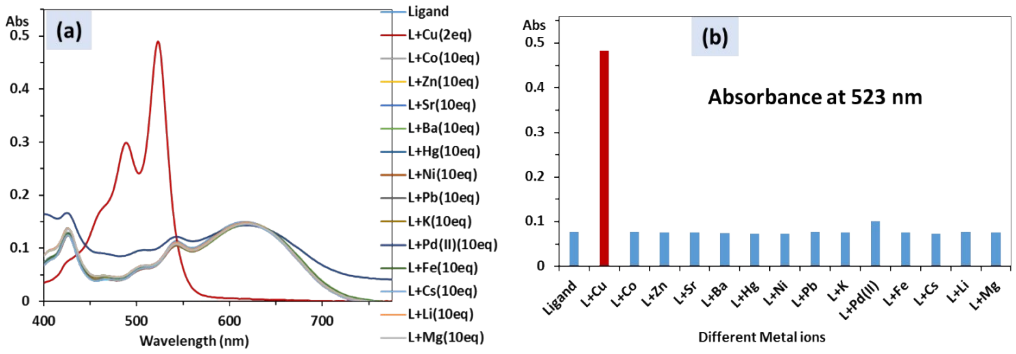

Figure S5. (a) Absorbance changes and (b) bar graph of **EA-PDI** (10 μM) on the addition of various metal ions (100 μM) recorded in HEPES–CH_3CN (1:1, pH 7.2) solution.

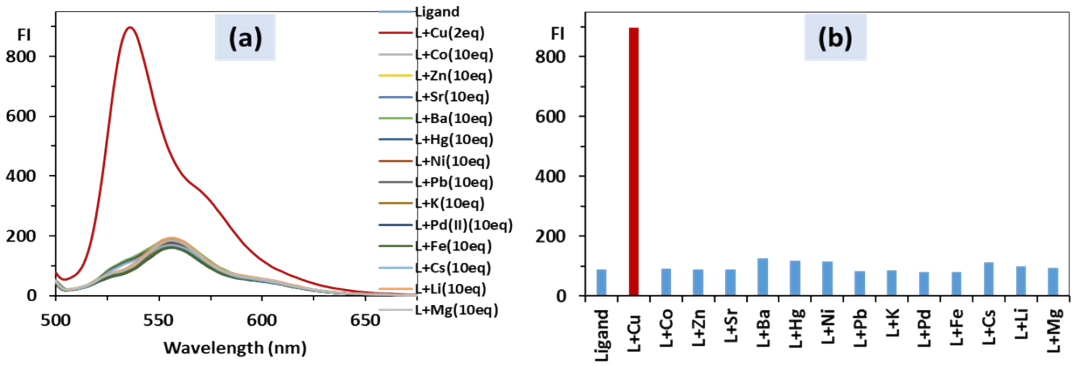

Figure S6. (a) Fluorescence changes and (b) bar graph of **EA-PDI** (0.05 μM) on the addition of various metal ions (100 μM) recorded in HEPES–CH_3CN (1:1, pH 7.2) solution.

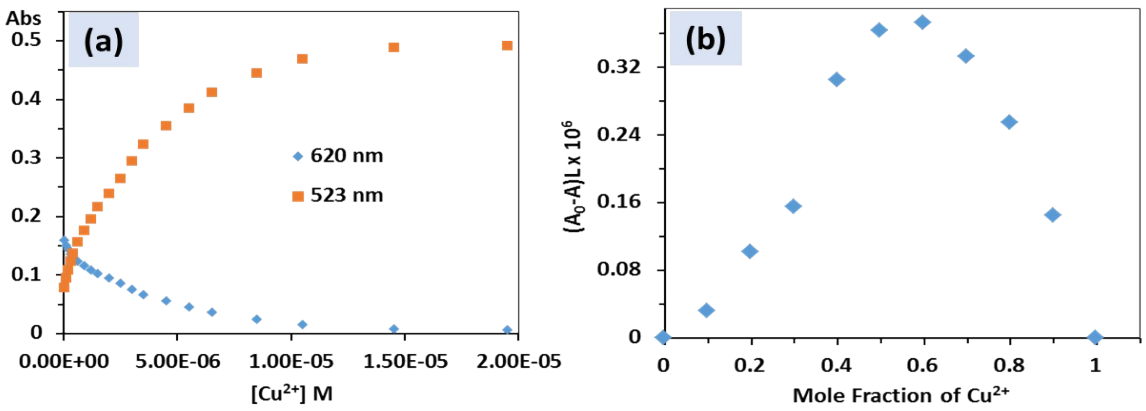

Figure S7. (a) Absorbance profile of **EA-PDI** (10 µM) recorded in HEPES buffer–CH_3CN (1:1, v/v, pH 7.2) on incremental addition of Cu^{2+} ions; (b) Job's plot of **EA-PDI** with increasing mole fraction of Cu^{2+} showing formation of 1:1 complex using UV-Vis Spectroscopy.

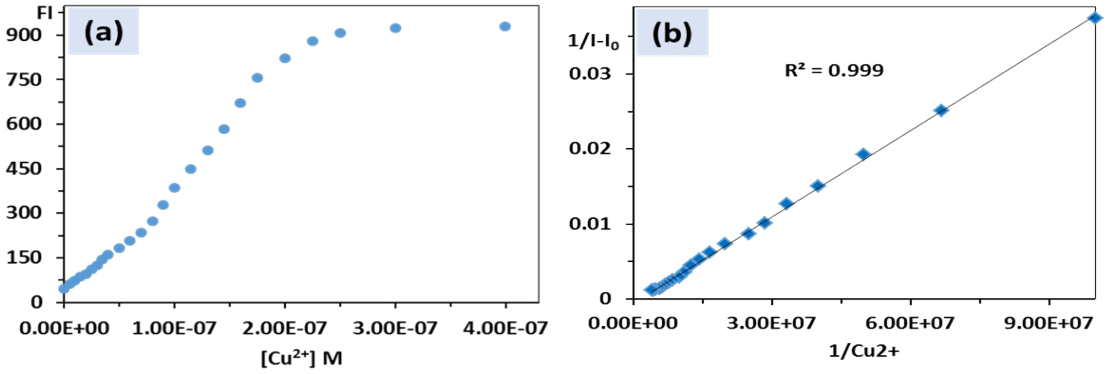

Figure S8. (a) Fluorescence profile of **EA-PDI** (0.05 µM) recorded in HEPES buffer–CH_3CN (1:1, v/v, pH 7.2) on incremental addition of Cu^{2+} ions; (b) Benesi-Hildebrand plot of **EA-PDI** in the presence of increasing concentrations of Cu^{2+} ions.

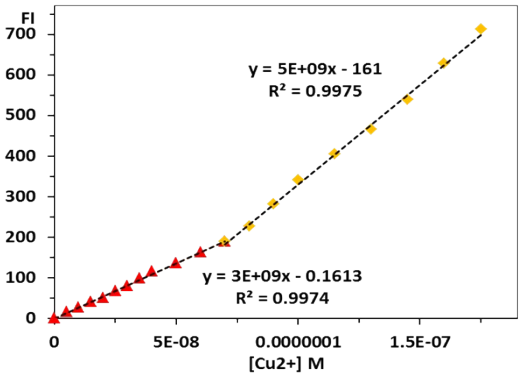

Figure S9. Plot of fluorescence intensity (FI) of **EA-PDI** (0.05 µM, 1:1 H_2O/CH_3CN vs Cu^{2+} ions.

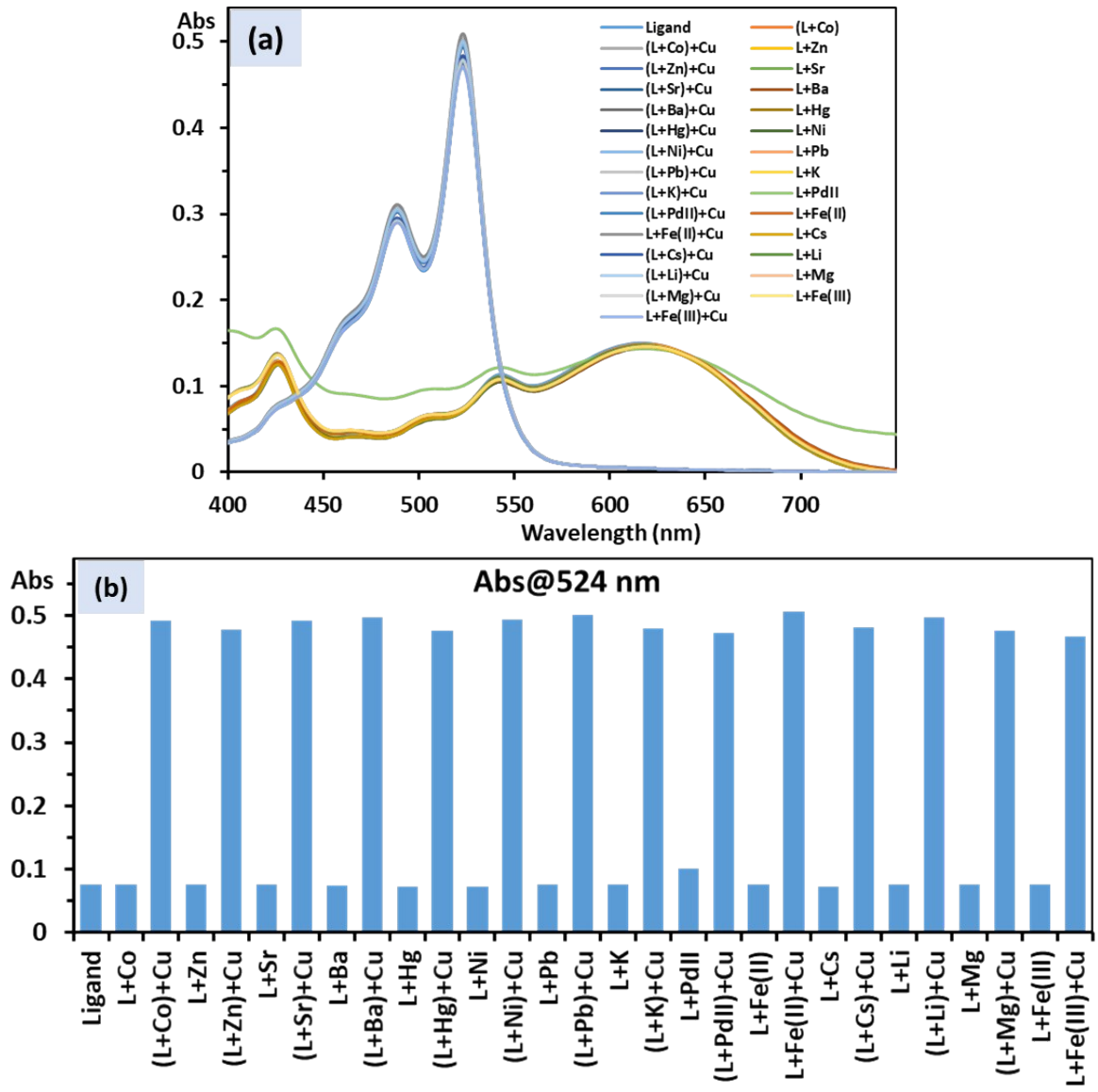

Figure S10. (a) Absorbance changes and (b) bar graph of **EA-PDI** (10 μM) on the addition of various metal ions (100 μM) and subsequently Cu^{2+} ions (20 μM) was added to check the interference and selectivity. All spectra were recorded in HEPES–CH_3CN (1:1, pH 7.2) solution.

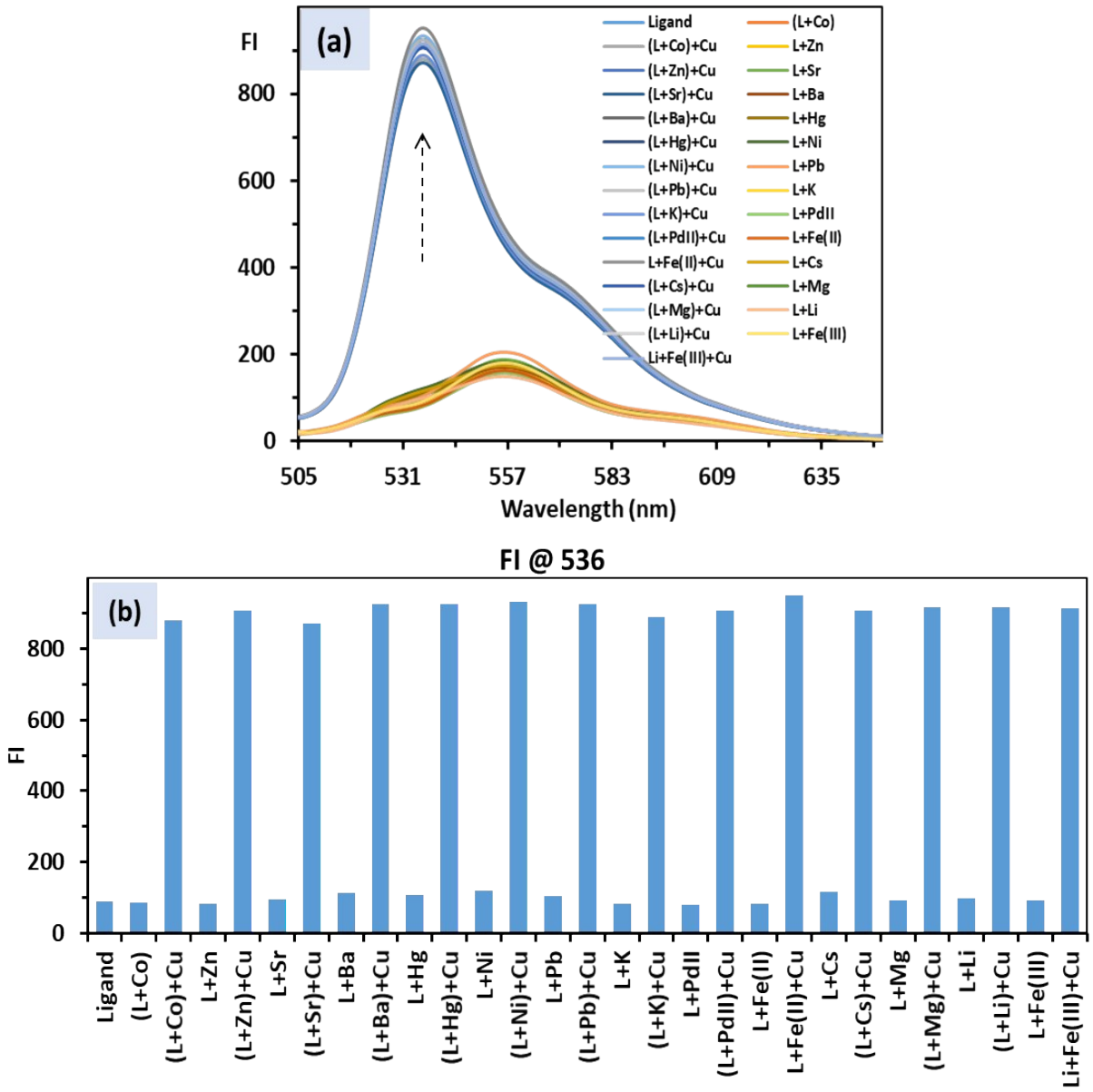

Figure S11. (a) Emission changes and (b) bar graph of **EA-PDI** (0.05 μM) on the addition of various metal ions (0.5 μM) and subsequently Cu^{2+} ions (0.1 μM) was added to check the interference and selectivity. All spectra were recorded in HEPES–CH_3CN (1:1, pH 7.2) solution. λ_{ex} = 490 nm, slit: 10 nm/7 nm.

Table S1: Photophysical parameters calculated for **EA-PDI**, **EA-PDI**∩Cu^{2+} complex and **EA-PDI**∩Cu^{2+} complex+spermine

Sr. No.	Photophysical parameter	**EA-PDI**	**EA-PDI**∩Cu^{2+} complex	**EA-PDI**∩Cu^{2+} complex+spermine
1.	Quantum Yield	11.5%	30.1%	11.2%
2.	Fluorescence life time	0.35 ns	0.7 ns	0.34 ns
3.	Radiative decay constant (K_r)	0.32x10^9/sec	0.43x10^9/sec	0.32x10^9/sec
4.	Non-radiative decay constant (K_{nr})	2.52x10^9/sec	0.184x10^9/sec	2.61x10^9/sec

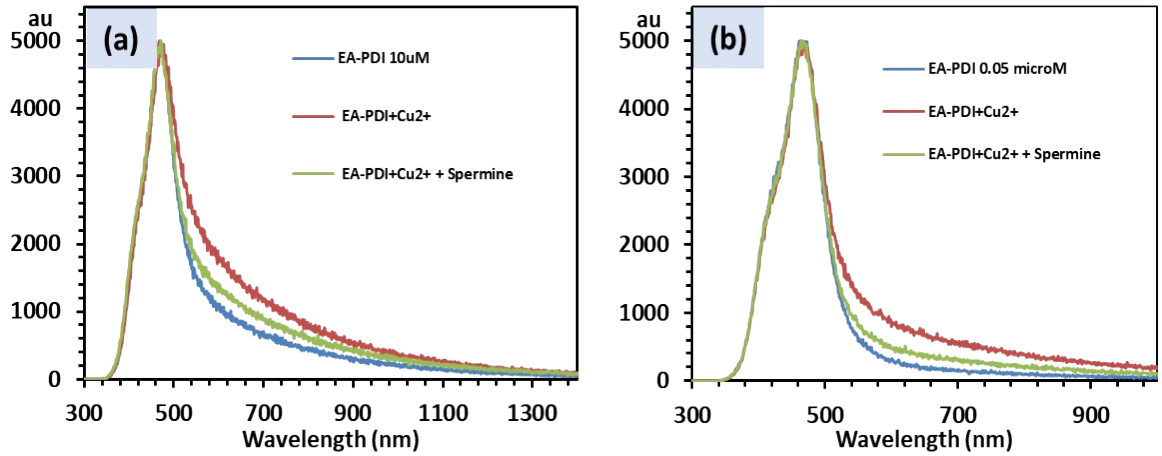

Figure S12. Fluorescence life time changes in (a) **EA-PDI** (10 µM) (b) **EA-PDI** (0.05 µM) on the addition of Cu^{2+} ions and subsequently spermine was added. All spectra were recorded in HEPES–CH_3CN (1:1, pH 7.2) solution.

5. Spectroscopic response of DGA-PDI towards Cu^{2+} ions

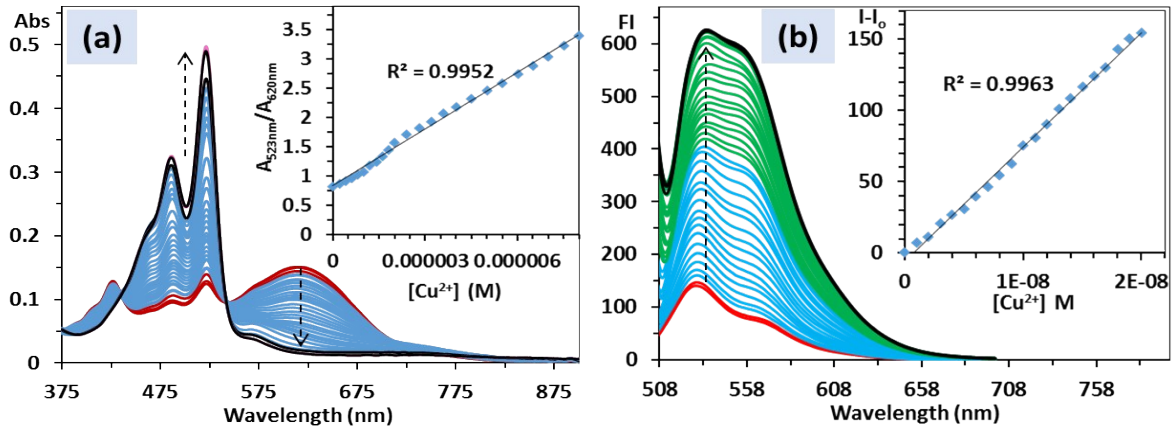

Figure 13. (a) Absorbance (10 μM) and (b) fluorescence spectra (0.05 μM) of **DGA-PDI** recorded on incremental addition of Cu^{2+} ions; [Inset] ratiometric plot between A_{523nm}/A_{620nm} versus concentrations of Cu^{2+}; [Inset] $I\text{-}I_o$ versus concentrations of Cu^{2+} for calculating the lowest detection limit.

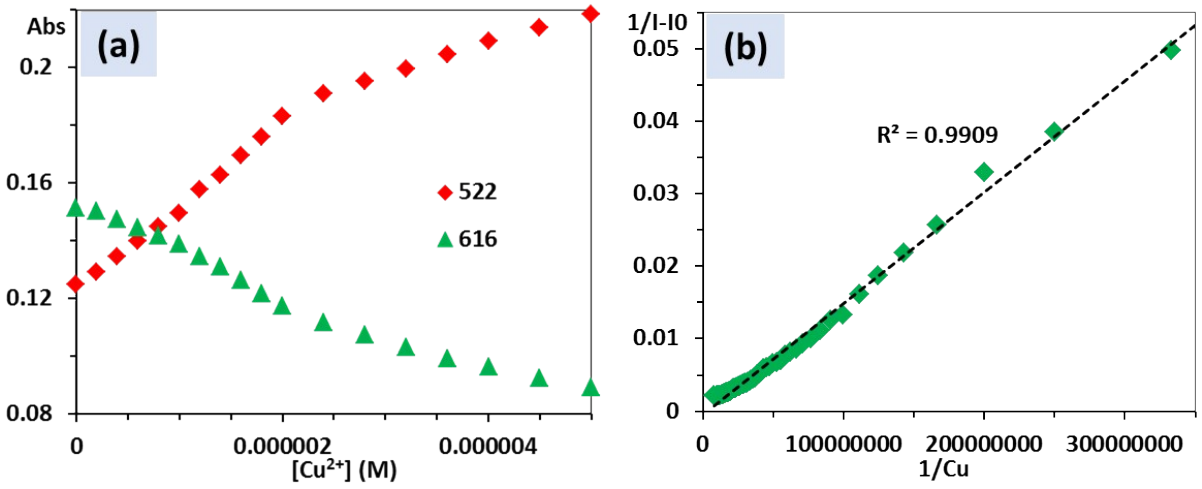

Figure S14. (a) Absorbance profiles of **DGA-PDI** (10 μM) recorded in HEPES buffer–CH_3CN (1:1, v/v, pH 7.2) on incremental addition of Cu^{2+} ions; (b) Benesi-Hildebrand plot of **DGA-PDI** in the presence of increasing concentrations of Cu^{2+} ions.

6. Detection of Cu^{2+} using TLC strip

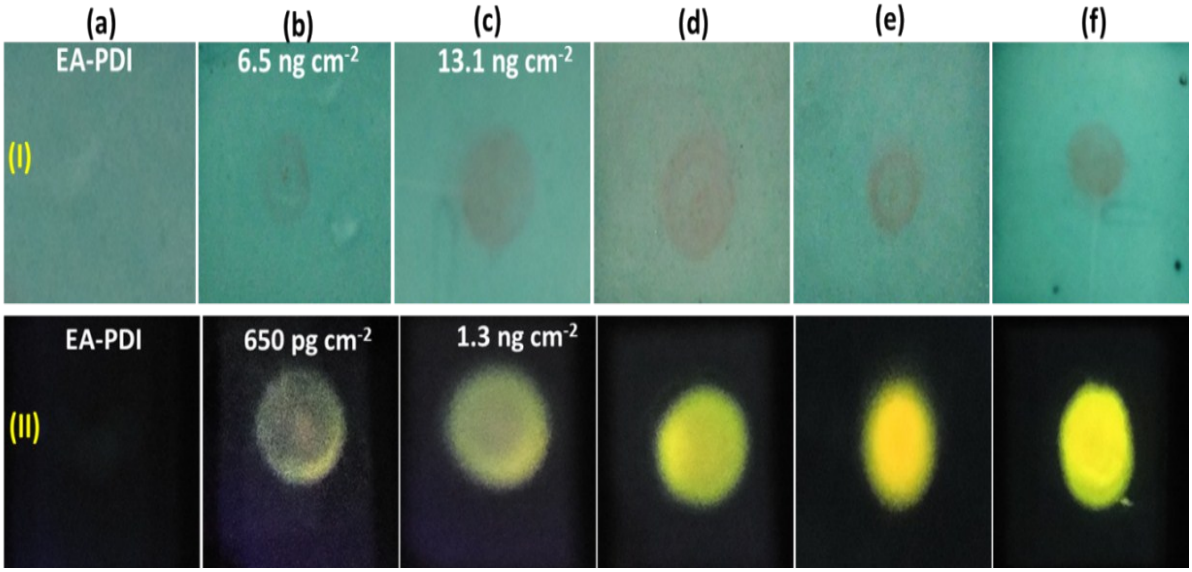

Figure S15. Colorimetric and fluorescent photographs of TLC strips coated with **EA-PDI** solution on addition of Cu^{2+} ions; (I) (a) TLC strip coated with **EA-PDI** ($2x10^{-5}$ M); TLC strips on addition of 5 µL of different concentration of Cu^{2+} ions (b) $5x10^{-6}$ M (c) $1x10^{-5}$ M (d) $2x10^{-5}$ M (e) $3x10^{-5}$ M and (f) $4x10^{-5}$ M; (II) (a) TLC strip coated with **EA-PDI** ($1x10^{-5}$ M); TLC strips on addition of 5 µL of different concentration of Cu^{2+} ions (b) $5x10^{-7}$ M (c) $1x10^{-6}$ M (d) $5x10^{-6}$ M (e) $1x10^{-5}$ M and (f) $2x10^{-5}$ M [The size of each TLC strip is 1 cm^2].

7. Detection of Cu^{2+} in biofluids (Blood Serum and Urine)

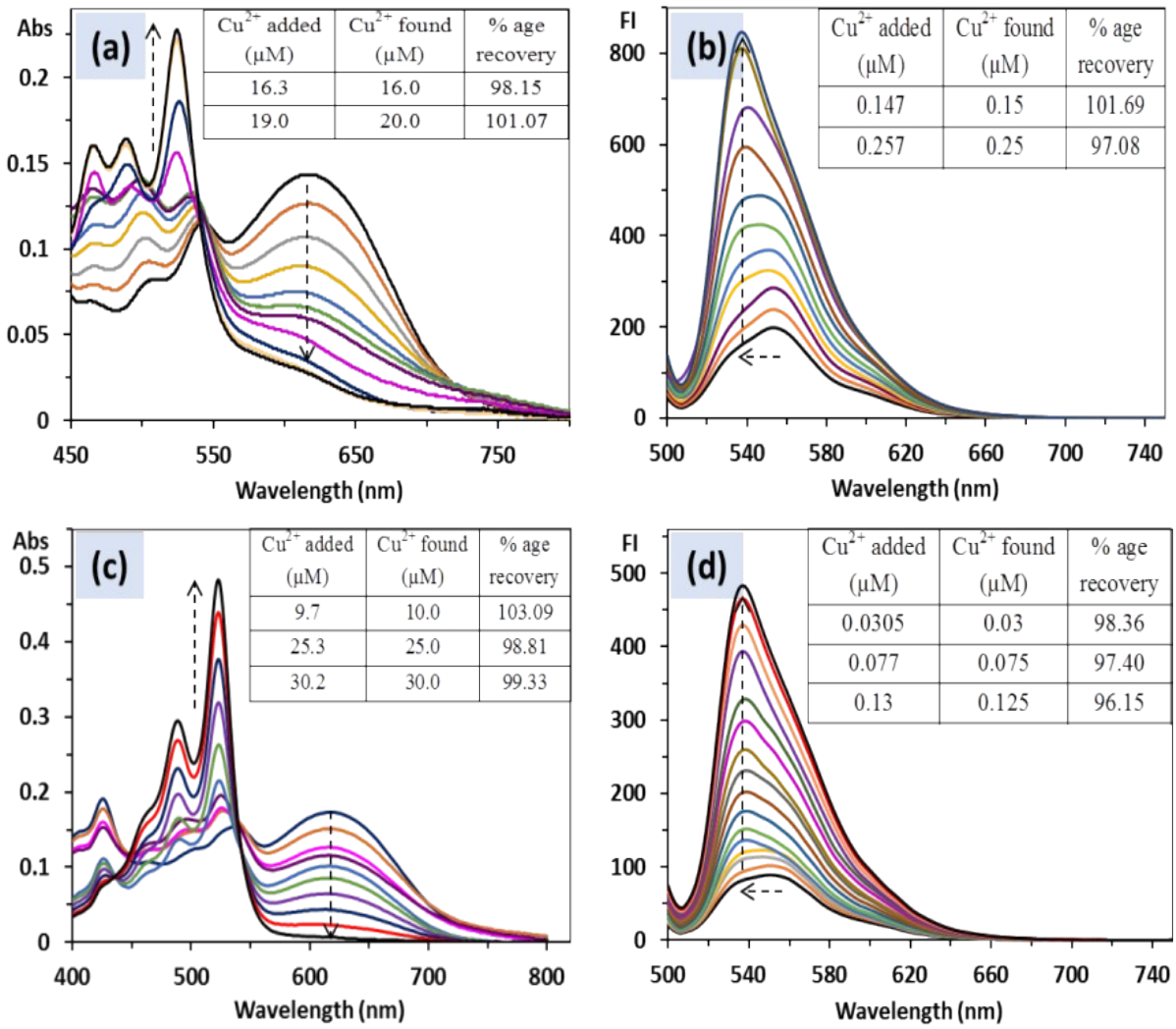

Figure S16. (a,c) Absorption and (b,d) fluorescence spectra of **EA-PDI** after the incremental addition of Cu^{2+} ions recorded in HEPES buffer-CH_3CN [1:1, v/v, pH 7.2, containing (a,b) 10% urine solution and (c,d) containing 10% blood serum]; inset in (a-d): table showing recovery of Cu^{2+} ions in spiked urine and blood serum samples.

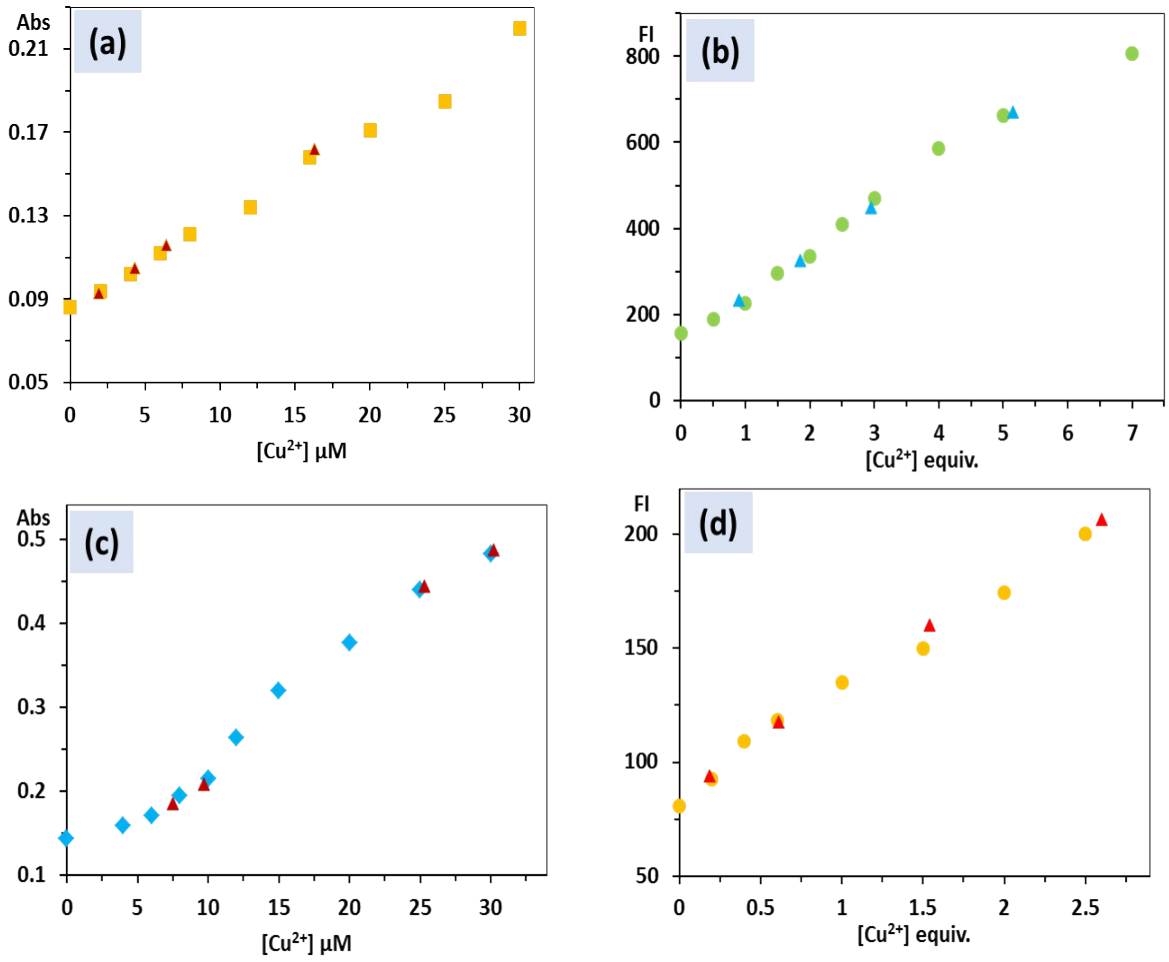

Figure S17. (a,c) Absorption and (b,d) fluorescence profile of **EA-PDI** after the incremental addition of Cu^{2+} ions recorded in HEPES buffer-CH_3CN [1:1, v/v, pH 7.2, containing (a,b) 10% urine solution and (c,d) containing 10% blood serum] along with recovery of spiked samples shown as colored points in each graph.

8. Effect of pH on EA-PDI and EA-PDI∩Cu^{2+}

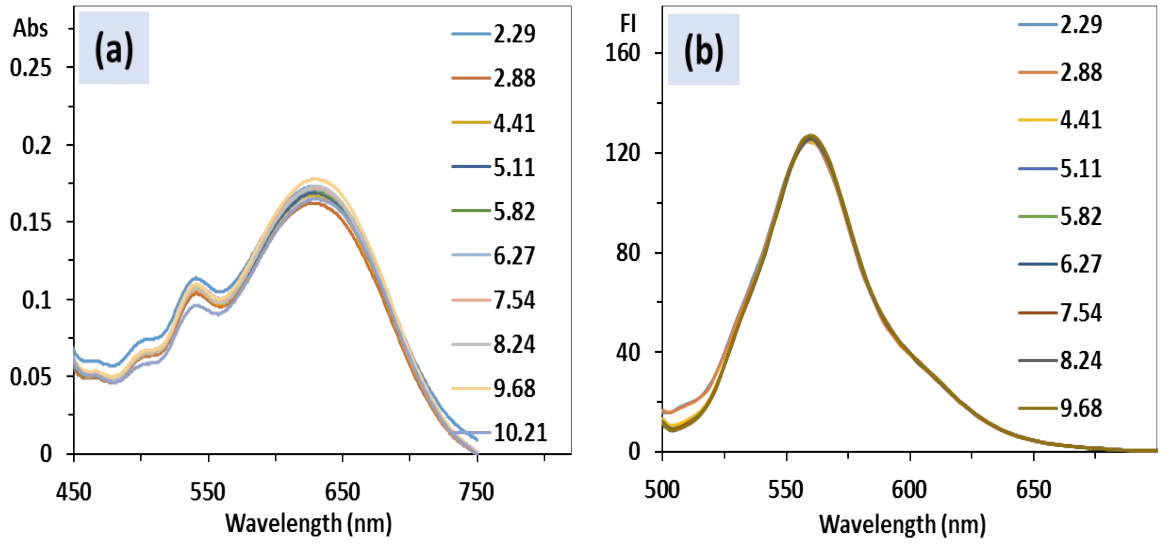

Figure S18. The effect of pH on the (a) absorbance and (b) fluorescence spectrum of **EA-PDI** (10 μM) recorded in CH_3CN:H_2O (1:1, v/v); λ_{ex} = 490 nm, slit: 15 nm/2.5 nm.

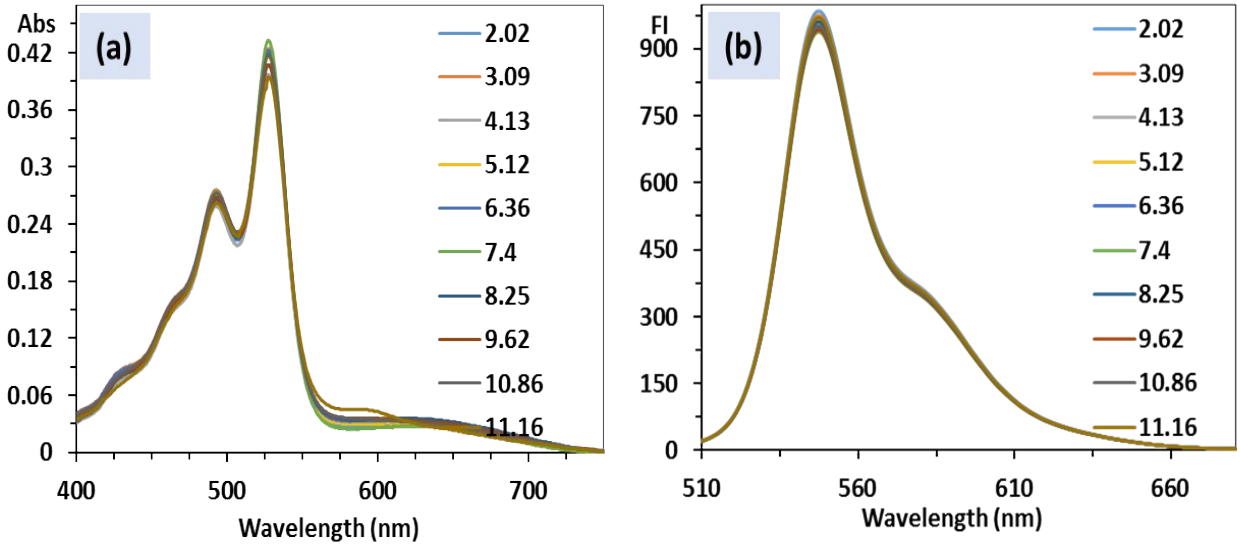

Figure S19. The effect of pH on the (a) absorbance and (b) fluorescence spectrum of **EA-PDI–**Cu^{2+} (10 μM) recorded in CH_3CN:H_2O (1:1, v/v); λ_{ex} = 490 nm, slit: 15 nm/2.5 nm.

9. Spectroscopic response of EA-PDI∩Cu^{2+} towards spermine

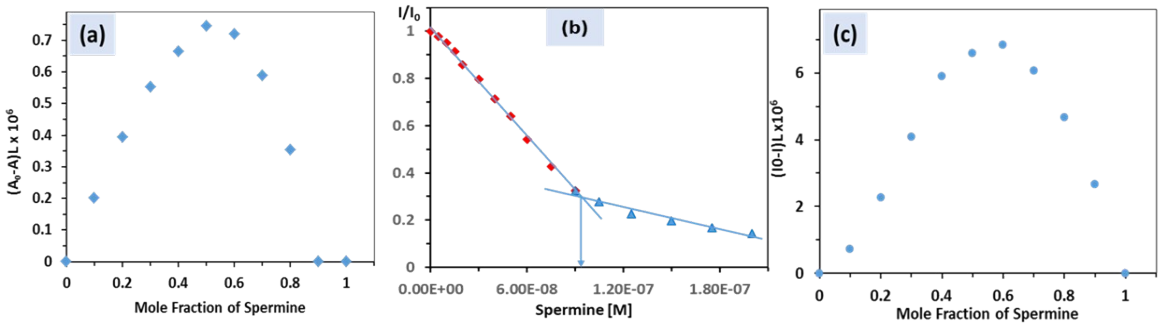

Figure S20. (a) Job's plot (absorbance) of **EA-PDI**–Cu^{2+} complex with spermine showing 1:1 stoichiometry; (b) Stern-Volmer (S-V) plot between I/I_o versus [spermine]; (c) Job's plot (fluorescence) of **EA-PDI**–Cu^{2+} complex with spermine showing 1:1 stoichiometry recorded in HEPES–CH_3CN (1:1, pH 7.2) solution.

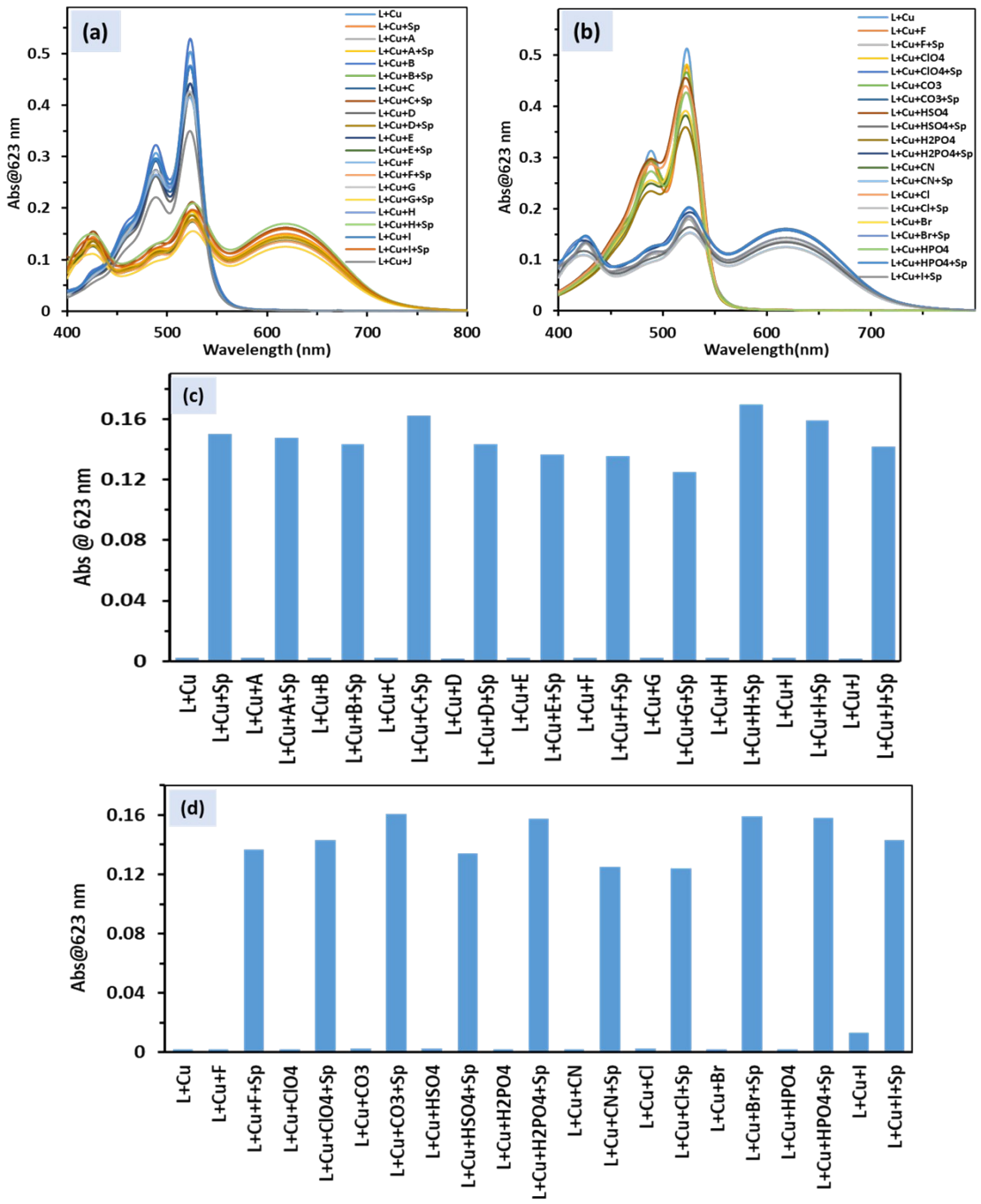

Figure S21. (a,b) Absorbance changes and (c,d) bar graph of **EA-PDI** (10 μM) on the addition of various amines and anions (100 μM) respectively and subsequently Cu^{2+} ions (20 μM) was added to check the interference and selectivity. All spectra were recorded in HEPES–CH_3CN (1:1, pH 7.2) solution. For Panel (a-d) Sp = Spermine; L = EA-PDI; EDTA (**A**), putrescine (**B**), tris(2-aminoethyl)amine (**C**), diethylenetriamine (**D**), 1,8-diaminoctane (**E**), 1,3-diaminopropane (**F**), phenylalanine (**G**); diethanolamine (**H**), N,N'-dimethyl ethylenediamine (**I**), spermidine (**J**). All these spectra were measured after 1-hour time gap.

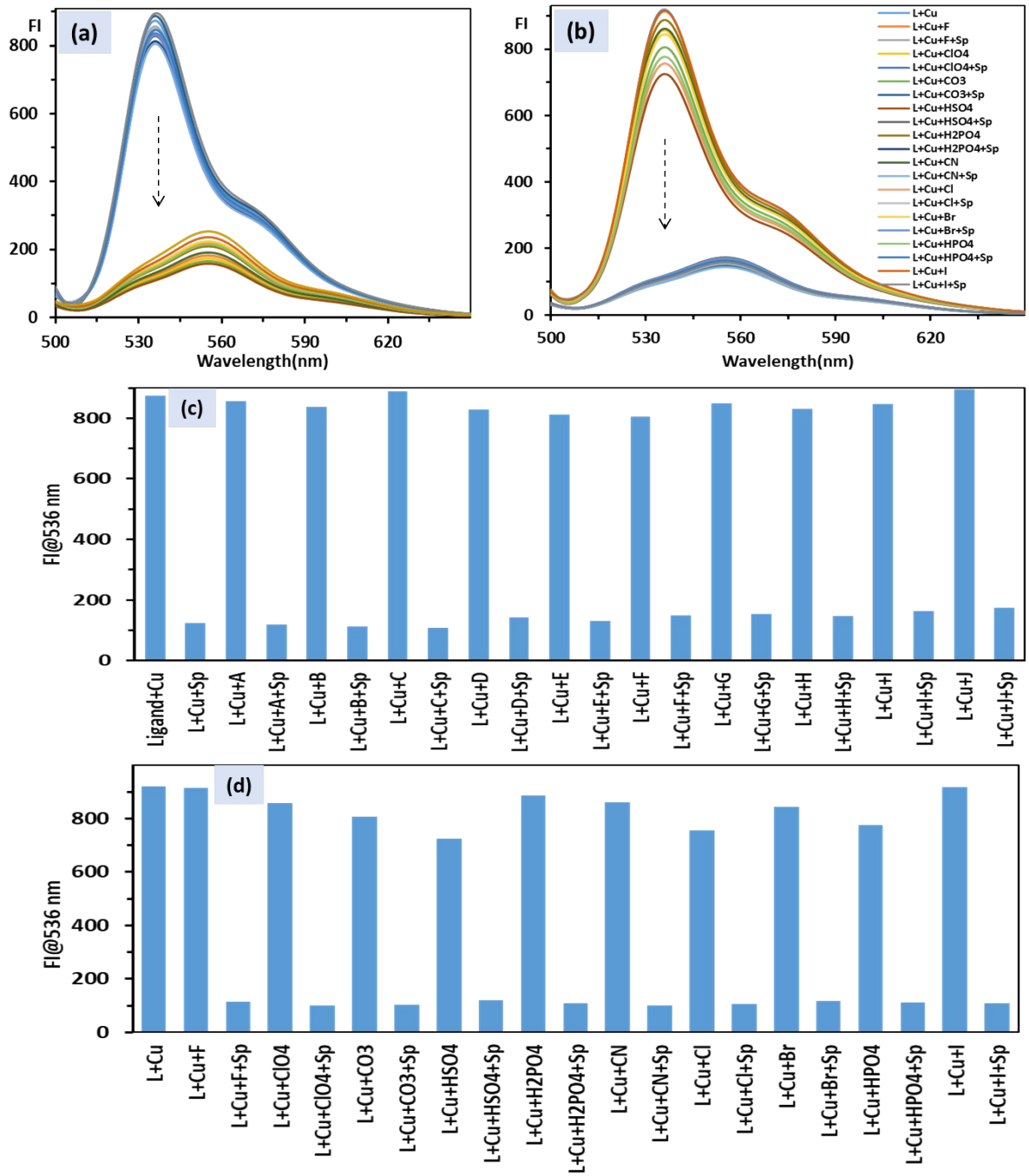

Figure S22. (a,b) Emission changes and (c,d) bar graph of **EA-PDI** (0.05 μM) on the addition of various amines and anions (0.5 μM) respectively and subsequently Cu^{2+} ions (0.1 μM) was added to check the interference and selectivity. All spectra were recorded in HEPES–CH_3CN (1:1, pH 7.2) solution. For Panel (a-d) Sp = Spermine; L = EA-PDI; EDTA (**A**), putrescine (**B**), tris(2-aminoethyl)amine (**C**), diethylenetriamine (**D**), 1,8-diaminoctane (**E**), 1,3-diaminopropane (**F**), phenylalanine (**G**); diethanolamine (**H**), N,N'-dimethyl ethylenediamine (**I**), spermidine (**J**). λ_{ex} = 490 nm, slit: 10 nm/7 nm. All these spectra were measured after 1-hour time gap.

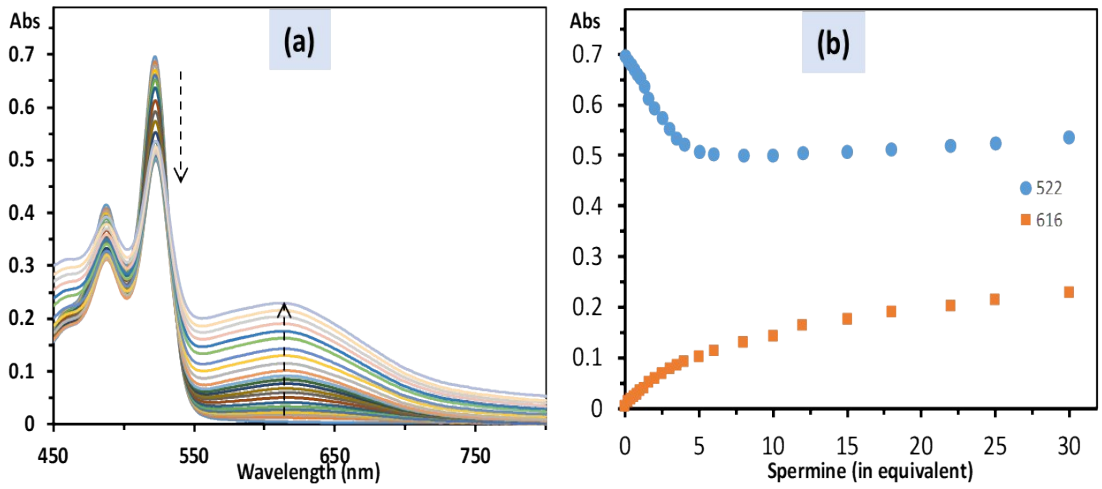

Figure S23. (a) Absorbance spectra of **DGA-PDI**∩Cu^{2+} complex showing detection of spermine in HEPES buffer-CH_3CN 7:3, v/v, pH 7.2 solution; (b) Plot of A_{616nm} and A_{522nm} versus concentrations of spermine. All spectra were recorded after time interval of 1 hour.

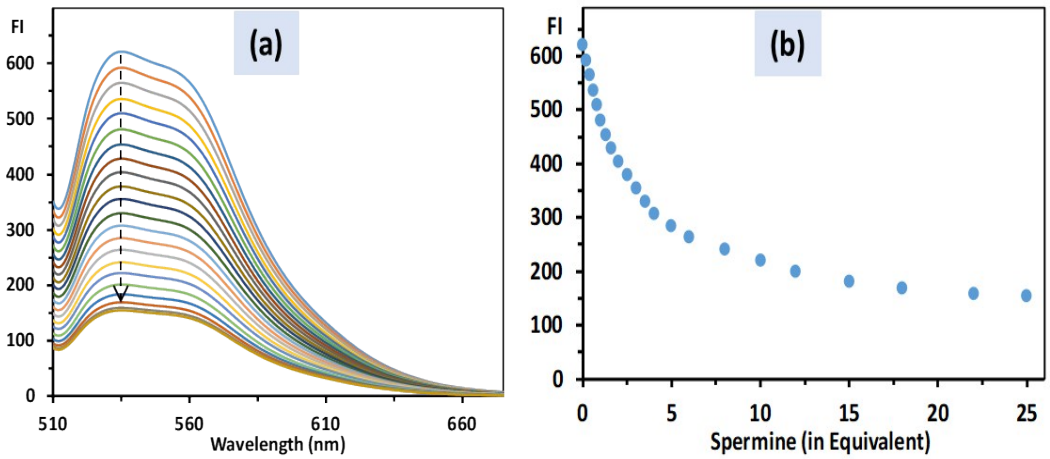

Figure S24. (a) Fluorescence spectra of **DGA-PDI**∩Cu^{2+} complex showing detection of spermine in HEPES buffer-CH_3CN 7:3, v/v, pH 7.2 solution; (b) Plot between A_{620nm}/A_{523nm} versus concentrations of spermine; λ_{ex} = 490 nm, slit: 10 nm/10 nm. All spectra were recorded after time interval of 1 hour.

10. Detection of spermine in biofluids using EA-PDI∩Cu^{2+} (Blood Serum and Urine)

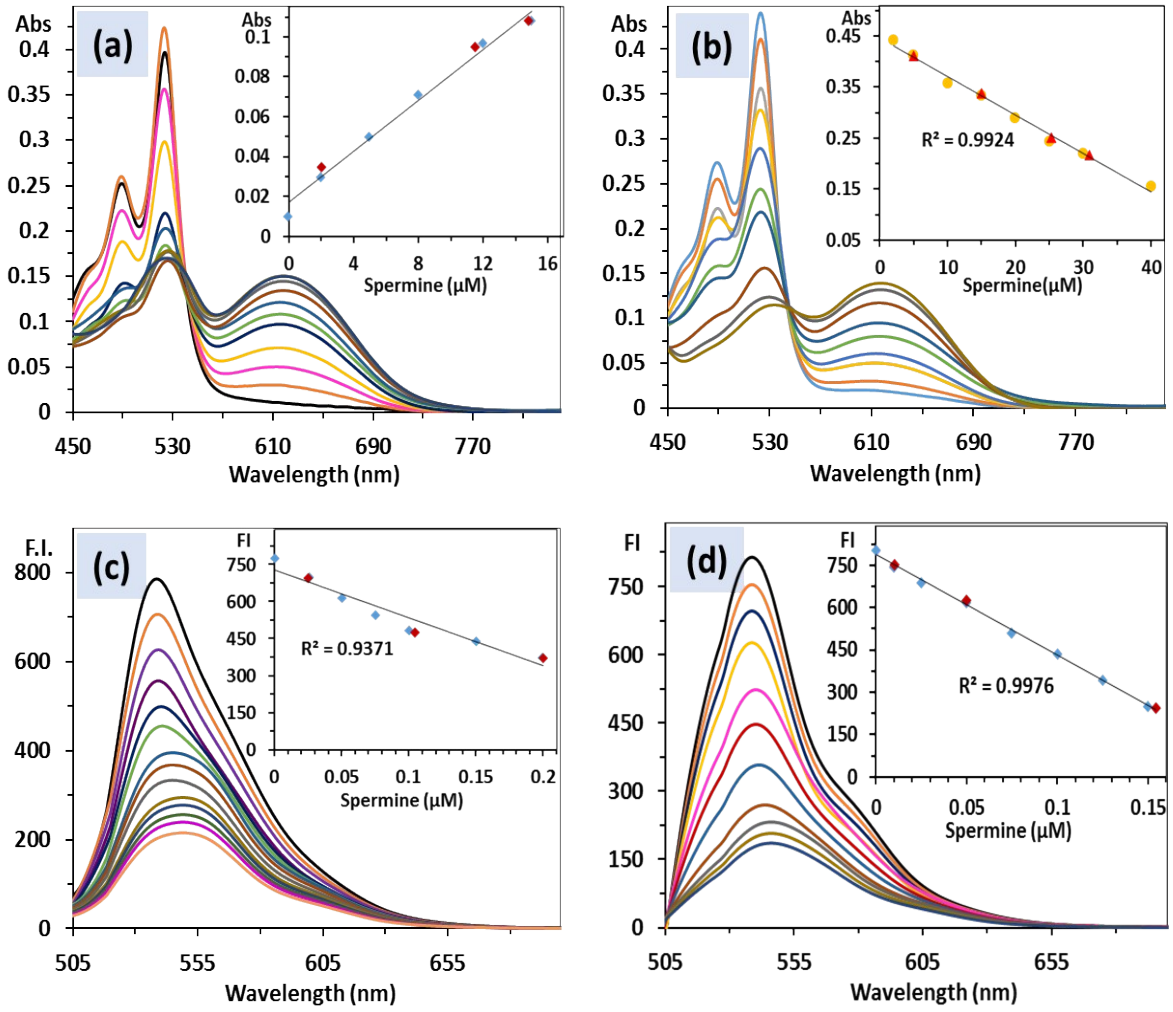

Figure S25. (a,b) Absorption and (c,d) fluorescence spectra e of **ENS** after the incremental addition of spermine recorded in HEPES buffer-CH_3CN [1:1, v/v, pH 7.2, containing (a,c) 10% urine solution and (b,d) containing 10% blood serum]; (Inset of a-c) graph showing the recovery of spermine

Table S2: Recovery of spermine using **EA-PDI∩Cu^{2+}** in spiked urine and blood serum samples recorded in HEPES buffer-CH_3CN [1:1, v/v, pH 7.2.

		Spermine		
Techniques	Samples	Spermine added (μM)	Spermine found (μM)	% age recovery
UV-Vis	**Blood Serum**	5.0	5.0	100
		15.0	15.0	100
		25.3	25.0	98.81
		30.9	30.0	97.08
	Urine	2.0	2.0	100
		11.5	12.0	104.34
		14.8	15.0	101.35
		40.0	40.0	100
Fluorescence	**Blood Serum**	0.0103	0.01	96.61
		0.05	0.05	100
		0.1545	0.15	97.08
		0.3	0.3	100
	Urine	0.0255	0.025	98.03
		0.105	0.1	95.69
		0.2	0.2	100
		0.4	0.4	100

11. Colorimetric diagomstic kit using EA-PDI∩Cu^{2+}

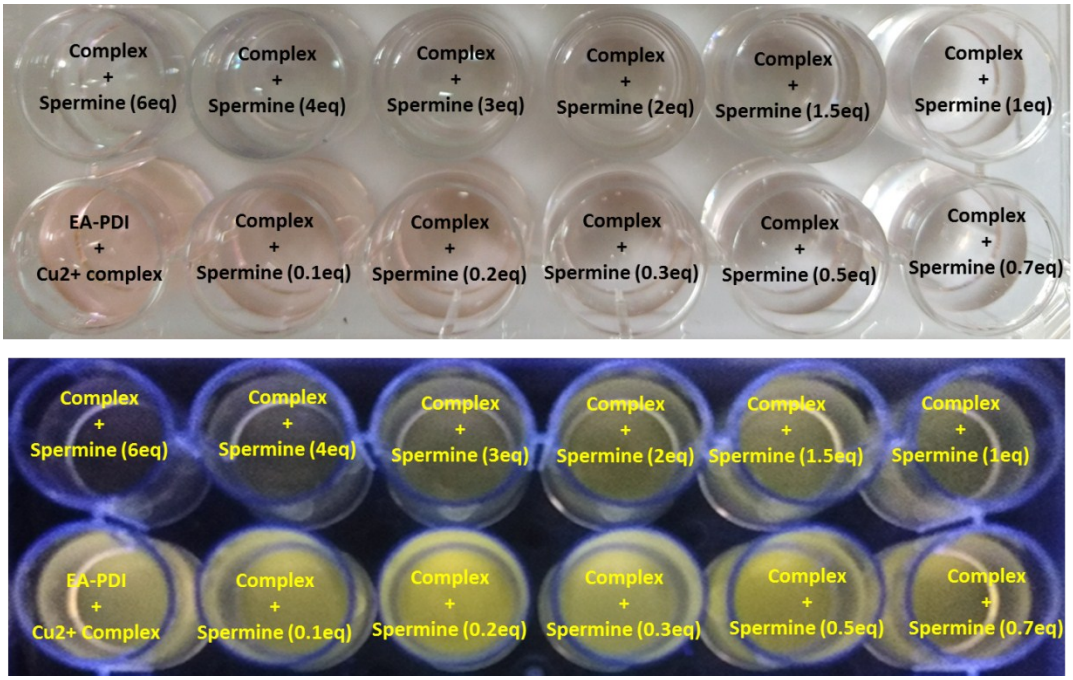

Figure S26. Fluorescence (λ_{ex} = 365 nm) images of well plate containing **ENS** (10 μM) alone (**1**) and **ENS** + different concentrations of spermine *viz.* 1 μM (**2**); 2 μM (**3**); 3 μM (**4**); 5 μM (**5**); 7 μM (**6**); 10 μM (**7**); 15 μM (**8**); 20 μM (**9**); 30 μM (**10**); 40 μM (**11**) and 60 μM (**12**).

12. Detection of spermine using TLC strip coated with EA-PDI∩Cu^{2+}

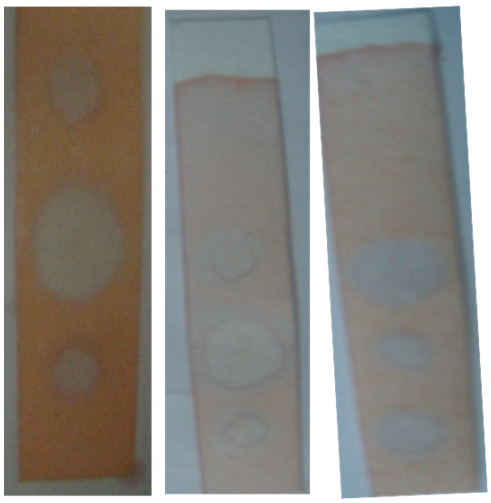

Figure S27. Detection of spermine by using **EA-PDI**+Cu^{2+} complex coated paper strips.

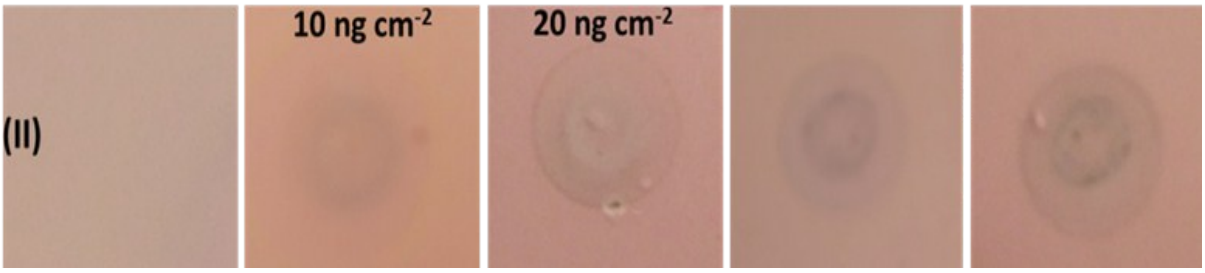

Figure S28. Colorimetric (50 μM) photographs of TLC strips coated with complex solution on addition of spermine; (II) (a) TLC strip coated with complex; TLC strips on addition of 5 μL of different concentration of spermine (b) $1x10^{-6}$ M (c) $5x10^{-6}$ M (d) $1x10^{-5}$ M and (e) $2x10^{-5}$ M [The size of each TLC strip is 1 cm^2].

13. Detection of spermine vapors in well plate using EA-PDI∩Cu^{2+}

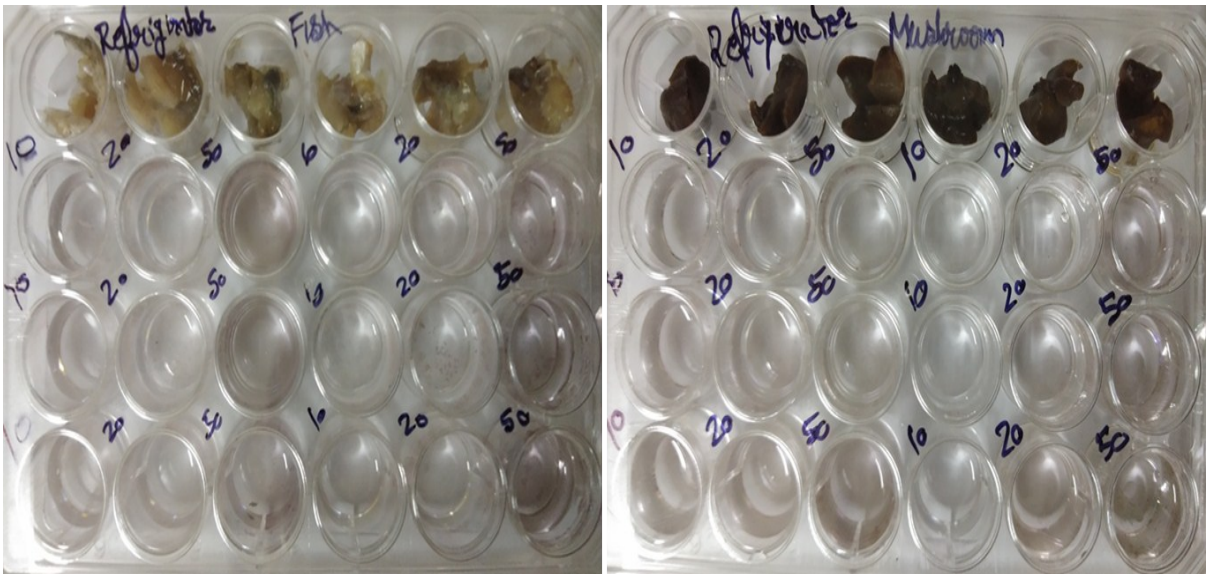

Figure S29. UV-Vis images of well plates kept at refrigeration conditions containing fish (F1-F3) and mushroom (M1-M3) samples in three wells of first row and rest of the wells in upper and lower images are filled with 10, 20 and 50 μM concentration of **EA-PDI**+Cu^{2+} complex (1:2) solution, respectively.

14. Detection of spermine in solution form using EA-PDI∩Cu^{2+}

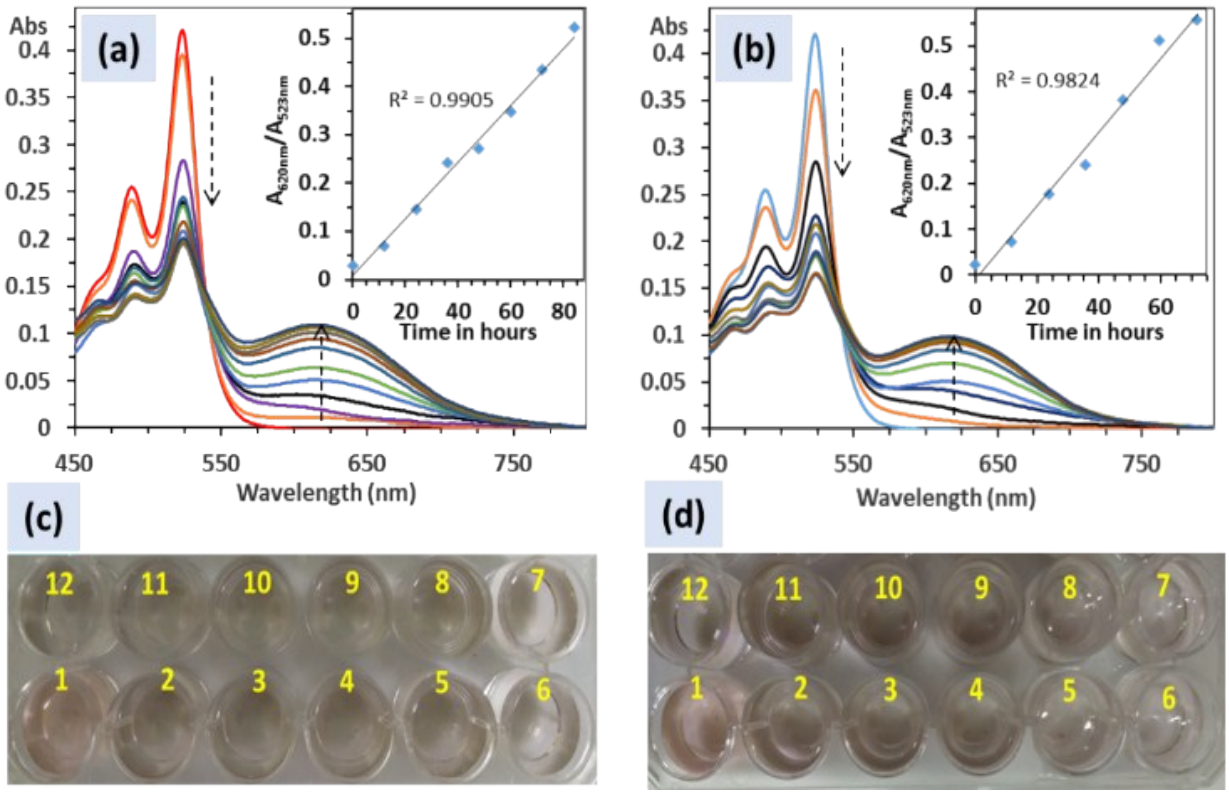

Figure S30. Absorbance spectra of complex showing detection of spermine in test samples collected from (a) fish and (b) mushroom; [Inset of (a) and (b)] ratiometric plot between A_{620nm}/A_{523nm} as function of time; Color images of well plate containing complex (**1**) and complex +test samples collected at different time interval (in hour) from (c) fish and (d) mushroom viz., 0 (**2**); 12 (**3**); 24 (**4**); 36 (**5**); 48 (**6**); 60 (**7**); 72 (**8**); 84 (**9**); 96 (**10**); 108 (**11**) and 120 (**12**).

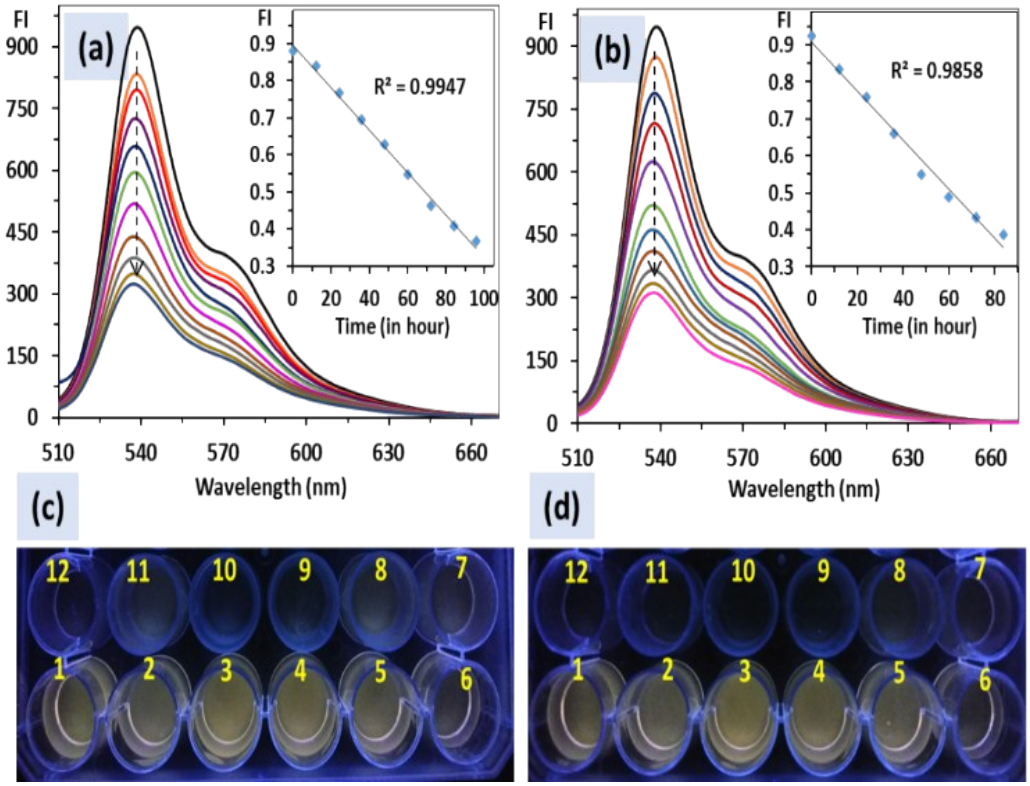

Figure S 31. Fluorescence spectra of complex showing detection of spermine in test samples collected from (a) fish and (b) mushroom; [Inset of (a) and (b)] plot of FI (I/I_o) as function of time; Color images of well plate containing complex (**1**) and complex +test samples collected at different time interval (in hour) from (c) fish and (d) mushroom viz., 0 (**2**); 12 (**3**); 24 (**4**); 36 (**5**); 48 (**6**); 60 (**7**); 72 (**8**); 84 (**9**); 96 (**10**); 108 (**11**) and 120 (**12**).

15. MTT assay and live cell imaging of Cu^{2+} using EA-PDI

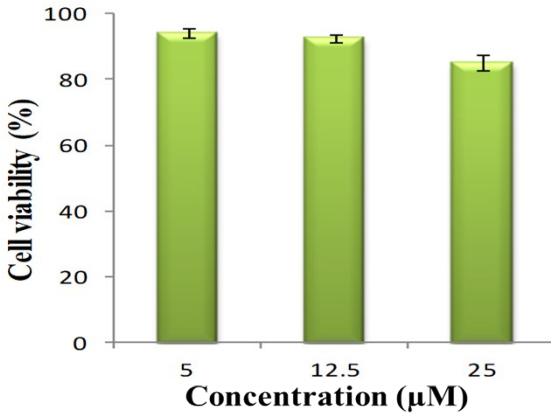

Figure S32. Cell viability values (%) tested by an MTT assay using MG-63 cells.

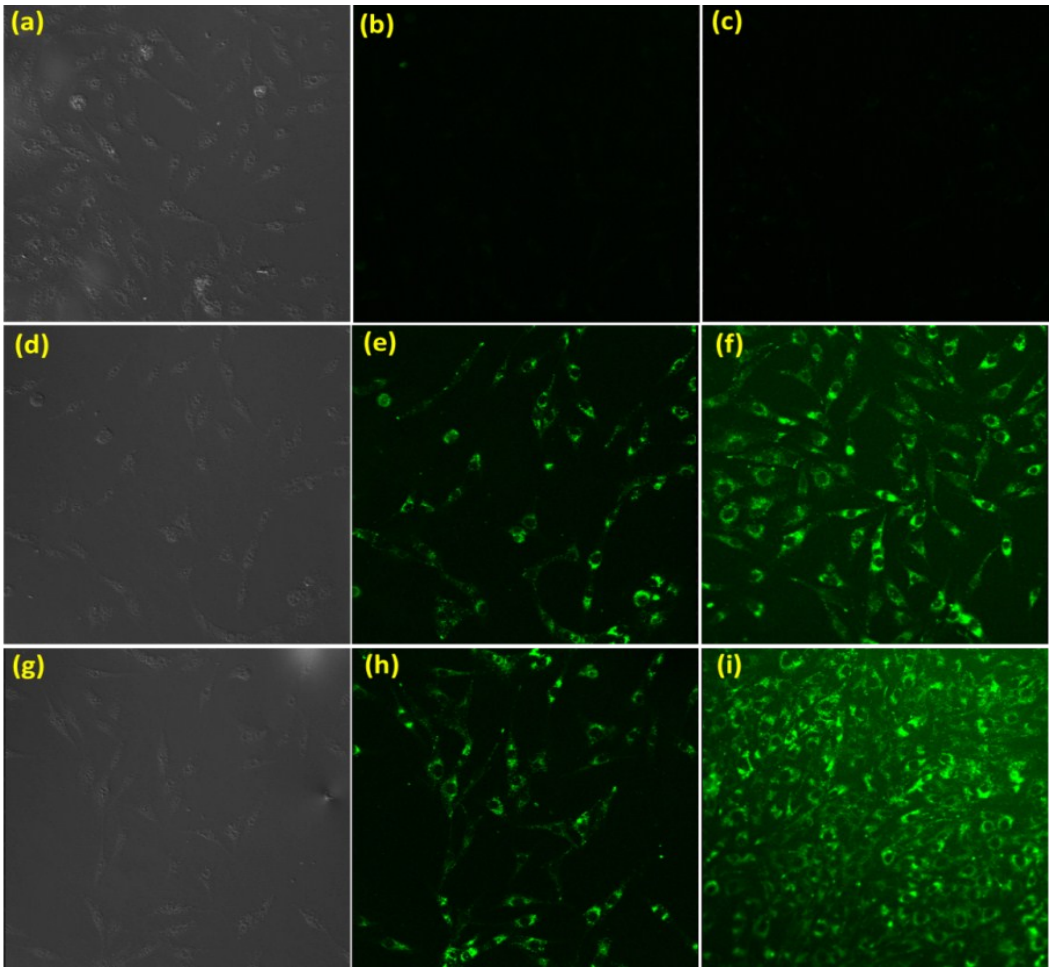

Figure S33: Brightfield image of MG-63 cells incubated with (a) **EA-PDI**; (d,g) **EA-PDI**–Cu^{2+}; fluorescence images of MG-63 cells incubated with (b) **EA-PDI** (1 μM) and (c) **EA-PDI** (5 μM) for 30 min; fluorescence image of MG-63 cells incubated with **EA-PDI** (1 μM) for 30 min and then incubated with (e) Cu^{2+} (4 μM) and (h) Cu^{2+} (8 μM) for another 30 min; fluorescence image of MG-63 cells incubated with **EA-PDI** (5 μM) for 30 min and then incubated with (f) Cu^{2+} (20 μM) and (i) Cu^{2+} (40 μM) for another 30 min.

16. Experimental Section

General methods: Chemicals and solvents were of reagent grade and used without further purification. All reactions were performed under N_2. CH_3CN, $CHCl_3$ and other solvents were of HPLC grade. Deionized water was obtained from ULTRA UV/UF Rions Lab Water System Ultra 370 series devices. Chromatographic purification was done with silica gel 60-120 mesh. TLC was performed on aluminium sheets coated with silica gel 60 F254 (Merck, Darmstadt). PDI **1** was synthesized according to literature procedures.

Instrumentation: ^1H and ^{13}C NMR spectra were recorded on a Bruker-AVANCE-II FT-NMR AL400 spectrometer using $CDCl_3$ as solvent. The peak values were obtained as ppm (δ), and referenced to tetramethylsilane (TMS) for ^1H NMR spectroscopy and the residual solvent signal for ^{13}C NMR spectroscopy. Data are reported as follows: chemical shifts in ppm, coupling constant *J* in Hz; multiplicity (s = singlet, bs = broad singlet, t = triplet, q = quartet, m = multiplet). The absorption spectra were recorded on a SHIMADZU-2450 spectrophotometer equipped with a Peltier system to control the temperature. Quartz cells of 1 cm in length were used for sample measurements. The spectral bandwidth and scan rate were fixed at 2 nm and 140 nm min^{-1} respectively. Fluorescence titrations were performed on a PerkinElmer LS-55 fluorescence spectrophotometers (slit width: excitation = 10 nm, emission = 7 nm) with excitation at 490 nm, unless otherwise stated. Quartz cells of 1 cm in length were used for sample measurements. FE-SEM measurements were performed on a ZEISS SUPRA^{TM}55 microscope operating at an acceleration voltage of 10 kV with a tungsten filament as the electron source. DLS measurements were performed at (25.0±0.1) ^oC by using a light-scattering apparatus (Zetasizer Nano ZS Malvern Instrument Ltd., UK). Solutions were filtered through a Millipore membrane filter (Acrodisc syringe filter, 0.45 μm Supor membrane) before measurements. The samples were thermally equilibrated for 10 min before each measurement, and an average of 10 measurement runs were considered to be data. The temperature was controlled to an accuracy of ±0.1 ^oC by using an in-built Peltier device. Data was analyzed by using standard algorithms.

Preparation of EA-PDI∩Cu^{2+} complex solution: 10 μM solution of **EA-PDI** for UV-Vis studies and 0.05 μM solution of **EA-PDI** for fluorescence studies were prepared in HEPES buffer–CH_3CN (1:1), v/v, pH 7.2 solution. These solution were treated with 2 equivalents of $Cu(ClO_4)_2$ and mixtures were allowed to stand for 1h at room temperature for equilibrium and then various UV-Vis, fluorescence, microscopic and light scattering measurements were taken.

Cell culture. Human Osteosarcoma MG-63 cell line was purchased from National Centre for Cell Science, Pune (India). Cells was grown routinely in DMEM (Dulbecco's Modified Eagle's Medium) supplemented with 10% (v/v) Fetal Bovine Serum (Biological Industries) and 1% antibiotic-antimycotic solution. The cells were cultured and maintained in CO_2 incubator in a 95% humidified atmosphere, 5% CO_2 and at 37°C in a tissue culture flask. Two wells served as control; cells of two wells were treated each with **EA-PDI** (1 and 5 μM prepared in CH_3CN:media, 5:95); Cu^{2+} ions (40 and 400 μM prepared in CH_3CN: media, 5:95) treatment was given to cells of two wells; 4 wells were treated with **EA-PDI** (2 wells each with 1 and 5 μM), cells of 8 wells were treated with **EA-PDI** (4 wells each with 1 and 5 μM) for 30 minutes followed by Cu^{2+} ions (2 wells each with 4 and 8 μM; 20 and 40 μM); cells of another 8 wells were treated with **EA-PDI** (2 wells each with 1 and 5 μM) for 30 minutes followed by Cu^{2+} ions (2 wells each with 4 and 8 μM; 20 and 40 μM) followed by treatment with spermine (16 and 32 μM; 80 and 160 μM). The cells were trypsinized and seeded in 24-well plates (1×10^5 cells/well) by placing 12 mm coverslip in each well. MG-63 cells were washed twice with 1xPBS and fixed with 4% paraformaldehyde for 10 minutes. After fixation, the cells were washed thrice with 1xPBS. The coverslips containing cells were mounted on the glass slides with anti-fading reagent (Fluoromount; Sigma). Finally, the images were captured by using Nikon A1R Laser Scanning Confocal Microscope system with an excitation of 490 nm. Imaging was performed with a 60x oil-emersion objective lens.

MTT Assay: The test sample was used to measure its cytotoxicity in Human Osteosarcoma MG-63 cell line using MTT assay with slight modifications. The cells were seeded at the concentration of $1x10^4$ cells/0.1 ml in a 96 well microplates and incubated for 24 hours to allow the adherence of cells. After attachment, the cells were treated with different concentrations of **EA-PDI**. After completion of another 24 hours, 20 μl of 3-(4,5-dimethylthiazol-2-yl)-2,5-diphenyltetrazolium bromide (MTT) was added in each well to determine the ability of viable cells to reduce it into purple colored formazan (insoluble) and the cells were incubated for 3-4 hours. Then the supernatant containing MTT solution was removed from each well and finally dissolved the intracellular formazan in 100 μl of dimethyl sulfoxide. The decrease in absorbance was read using a multiwell plate reader (BioTek Synergy HT) at 570 nm.

Sample preparation for TLC Strips. TLC strips were made by dipping 1 cm x 1 cm aluminium sheets coated with silica gel 60 F254 into 20% water–CH_3CN solution of **EA-PDI** (10 μM for fluorescence; 50 μM for colorimetric methods) solution followed by drying at room temperature.

Different concentrations of Cu^{2+} or spermine were prepared in aqueous solution. One drop containing 5 μL aliquot of each solution of different concentrations of Cu^{2+} was added on the TLC strips previously coated with **EA-PDI** and dried before visualization under UV lamp. After that one drop containing 5 μL aliquot of each solution of different concentrations of spermine was added on the same area of TLC strip where drop of Cu^{2+} was deposited. After drying, the area where spermine was added again visualized under UV lamp to produce all the images. For control experiment, drop of water alone was also added on the same area of TLC strip where drop of Cu^{2+} was deposited. The TLC strips were then visualized under sunlight or UV irradiation (365 nm lamp).

Preparation of urine and blood serum samples. For estimation of Cu^{2+} and spermine in the clinical samples, blood serum and urine from healthy humans were collected from health center of the university with the consent of donors. The permission for experiments with blood serum and urine samples was accorded by the Institutional Ethical Committee, Guru Nanak Dev University (letter No. 661/HG dated 29-3-2016). We prepared solution of **EA-PDI** and **EA-PDI**∩Cu^{2+} complex (1:2) in HEPES buffer–CH_3CN (1:1) containing 10% urine or blood serum and independently spiked with known concentrations of Cu^{2+} and spermine, respectively in the range of 0–40 μM concentrations. The absorbance and fluorescence spectra of these Cu^{2+} and spermine spiked solutions were recorded and compared with standard calibration curves.

Detection of biogenic amine (spermine) in food samples. A fresh mushroom and fish samples were procured from a local market and washed with distilled water. Immediately a series of three samples in duplicates for fish and mushroom (2 g/well) were separately kept in 24-well plates and the remaining wells were filled with 1 mL of **EA-PDI**∩Cu^{2+} complex solution of different concentrations such as 10, 20 and 50 μM. The cover was placed on the well plates and were kept in different storing conditions, i.e., room temperature and frozen temperature (0 °C). The photographs were taken after duration of 3 and 6 days. In another experiment, fish and mushroom samples were separately sealed in a 50 mL glass container and 30 mL of water was added and samples were sealed with aluminium foil and kept at room temperature. The solutions (1.0 mL) using microsyringe were collected at regular time intervals over a period of 120 h from each sample and injected into HEPES buffer–CH_3CN (1:1, v/v pH 7.2) solution of **EA-PDI**∩Cu^{2+} complex (1:2). After equilibrium was reached, absorbance (A_{620nm}/A_{523nm}) and fluorescence (I/I_o) responses of **EA-PDI**∩Cu^{2+} complex was recorded as a function of time.

Table S3: Comparison of the present manuscript with literature reports

Sr. No.	Citation	Type of system	Solvent system	Detection limits	Live cell imaging	Detection in clinical samples	Detection in Food products (aqueous systems)	Detection in food products (vapour phase)	Solid state detection
	Present manuscript	**Perylenediimide and Cu^{2+} complex based nanoparticles**	**HEPES: CH_3CN (1:1)**	**86.3 nM (UV-vis) and 90 pM (FI) in aqueous medium**	**Confocal Imaging of Cu^{2+} and spermine in human Osteosarcoma MG-63 cells**	**Human urine and blood serum samples**	**Fermented Meat and Mushroom samples**	**Fermented Meat and Mushroom samples**	**Test strips-based detection method (detection limits 0.1 µg/L)**
1.	Sensor Actuator B Chem: 2018, 270, 552-561	1-(2-naphthyl)benzimidazolium + SDS	95% HEPES Buffer	6 nM	No	Yes	No	No	No
2.	ACS Sustainable Chem. Eng.2017, 5, 1287−1296	Cu^{2+} complex of organic nanoparticles	DMF(1): H_2O(99)	36.2 (UV-Vis)	No	No	No	Food articles (Mushroom and meat)	No
3.	Anal. Chem.2014, 86, 1347−1351	Gold nanoparticles	-	10 ppb	No	Human urine samples	No	No	No
4.	Biosensors and Bioelectronics, 2017, 88, 71-77	Tyrosine-Au NPs	Aqueous system	136 pM (UV-Vis) and 6.2 nM(FI)	No	Human plasma and urine samples	No	No	No
5.	Eur. J. Inorg. Chem.2015, 4437–4442	Dipicolinic acid hydrazide Schiff base	Aqueous system	7.26 nM (UV)	No	Real samples analysis	No	No	No
6.	Anal. Chem.2016, 88, 7358−7364	Polymer-surfactant complexation	Aqueous system	0.33 µM/66 ppb	No	Human urine samples	No	No	No
7.	Sensors and Actuators B 257 (2018) 734–744	amphiphilc thiophene copolymers coated CdTe QDs	PBS Buffer	2.90 nM and 1.66 nM (FI)	No	Human serum samples	No	No	No
8.	Chem. Commun.,2016,52, 1040-1043	Micelles of pyrene and squaraine	Buffered solutions	4.73 µM	No	Human Urine samples	No	No	Test strips method
9.	Chem. Commun.,2016,52,10648-10651		Buffered solutions	0.6 µM (FI)	No	Artificial urine samples	No	No	No
10.	Chem. Asian j. 2017, 12, 890-899	Perylene-SDS self-assemblies for spermine	HEPES:CH_3CN(1:1)	27.5nM (FI)	No	urine and blood serum samples	No	No	Test strips method